Secreted long non-coding RNAs *Gadlor1* and *Gadlor2* aggravate cardiac remodelling during pressure overload by affecting multiple cardiac cell types

Merve Keles[1,2,3]*, Steve Grein[1,3]*, Natali Froese[4], Dagmar Wirth[5], Felix A. Trogisch[1,2,3], Rhys Wardman[1,3], Shruthi Hemanna[1,3], Nina Weinzierl[1], Philipp-Sebastian Koch[6], Stefanie Uhlig[7], Santosh Lomada[3,8], Gesine M. Dittrich[1,3], Malgorzata Szaroszyk[4], Ricarda Haustein[4], Jan Hegermann[9], Abel Martin-Garrido[1], Johann Bauersachs[4], Derk Frank[10, 11], Norbert Frey[3,12], Karen Bieback[7], Julio Cordero[13], Gergana Dobreva[3,13], Thomas Wieland[3,8] and Joerg Heineke[1,2,3]

[1]ECAS (European Center for Angioscience), Department of Cardiovascular Physiology, Medical Faculty Mannheim of Heidelberg University, Mannheim, Germany;

[2]CFPM (Core Facility Platform Mannheim), Cardiac Imaging Center, Medical Faculty Mannheim of Heidelberg University, Mannheim, Germany;

[3]DZHK (German Center for Cardiovascular Research), partner site Heidelberg/Mannheim, Germany;

[4]Department of Cardiology and Angiology, Hannover Medical School, Hannover, Germany;

[5]Helmholtz Centre for Infection Research, Model Systems for Infection and Immunity, Braunschweig, Germany;

[6]Department of Dermatology, Venereology and Allergology, University Medical Center and Medical Faculty Mannheim, Heidelberg University, Mannheim, Germany;

[7]CFPM, FlowCore, Medical Faculty Mannheim of Heidelberg University, Mannheim, Germany;

[8]ECAS, Department of Experimental Pharmacology, Medical Faculty Mannheim of Heidelberg University, Mannheim, Germany;

[9]Institute of Functional and Applied Anatomy, Core Unit Electron Microscopy, Hannover Medical School, Hannover, Germany;

[10]Department of Internal Medicine III, University Hospital Schleswig-Holstein, Kiel, Germany;

[11]DZHK, partner site Hamburg/Kiel/Lübeck

[12]Department of Internal Medicine III, Medical Faculty Heidelberg, Heidelberg University, Heidelberg, Germany;

[13]ECAS, Cardiovascular Genomics and Epigenomics, Medical Faculty Mannheim of Heidelberg University, Mannheim, Germany.

*these authors contributed equally.

Address for Correspondence:

Prof. Dr. Joerg Heineke

Department of Cardiovascular Physiology

European Center for Angioscience (ECAS)

Medical Faculty Mannheim, Heidelberg University

Ludolf-Krehl-Straße 7 – 11

68167 Mannheim, Germany

Phone: +49 621 383 71850

Email: Joerg.Heineke@medma.uni-heidelberg.de

Short title: *Gadlor1* and *Gadlor2* lncRNAs during Cardiac Remodelling

Abstract

Aims: Pathological overload triggers maladaptive myocardial remodelling that leads to heart failure. Recent studies have shown that long non-coding RNAs (lncRNAs) contribute to the development of cardiac disease. This study investigates two related, recently discovered, secreted lncRNAs, *Gadlor1* and *Gadlor2*.

Methods and Results: In the heart, *Gadlor1/2* are mainly expressed in endothelial cells and to a lesser extent in fibroblasts. *Gadlor1/2* are upregulated in failing mouse hearts as well as in the myocardium and serum of heart failure patients. Interestingly, *Gadlor1/2* are secreted from endothelial cells within EVs and affect multiple cell types. *Gadlor* knock-out and overexpression during experimental cardiac pressure overload by transverse aortic constriction (TAC) was analysed.

Gadlor-KO mice exhibited reduced cardiomyocyte hypertrophy, diminished myocardial fibrosis and improved cardiac function, but paradoxically suffered from sudden death during prolonged overload. *Gadlor* overexpression, in turn, aggravated hypertrophy, fibrosis and cardiac dysfunction during TAC. Mechanistically, *Gadlor1/2* inhibited angiogenic gene expression in endothelial cells, while promoting the expression of pro-fibrotic genes in cardiac fibroblasts. We employed RNA antisense purification coupled with mass spectrometry and identified the calcium/calmodulin-dependent protein kinase type II (CaMKII) as interaction partner of *Gadlor1/2* in cardiomyocytes (CM). By activating CaMKII, *Gadlor1/2* promote hypertrophic gene-expression and affect excitation-contraction coupling in these cells.

Conclusion: The lncRNAs *Gadlor1* and *Gadlor2* are upregulated in mouse and human hearts during pathological overload. Because they are secreted within EVs, they affect multiple cardiac cell types and inhibit angiogenesis, induce myocardial fibrosis, hypertrophy as well as alterations in calcium homeostasis in CMs.

Key words: Long non-coding RNA – Extracellular vesicles – Heart failure – Hypertrophy – Pressure overload - calcium/calmodulin-dependent protein kinase type II

Structured Graphical Abstract

Key Question:

Long non-coding RNAs are potent regulators of cardiac diseases. In this study, we aimed to decipher the role of two recently identified long non-coding RNAs, *Gadlor1* and *Gadlor2,* in cardiac remodelling during pressure overload.

Key Findings:

Gadlor1/2 are two lncRNAs mainly secreted from endothelial cells in extracellular vesicles, which are taken up by cardiomyocytes. *Gadlor1/2* are also expressed in fibroblasts. *Gadlor1/2* are upregulated in failing mouse and human hearts and trigger cardiac hypertrophy, fibrosis and failure.

Take Home Message:

Gadlor1 and *Gadlor2* are secreted and conserved lncRNAs, which are highly induced in patients suffering from heart failure, when they are associated with reduced cardiac function and might constitute a new therapeutic target.

1 **Translational Perspective**

2 Here, we characterized two secreted lncRNAs *Gadlor1/2*, which are conserved in humans. We
3 observed a negative correlation between *GADLOR2* serum levels and left ventricular ejection
4 fraction in heart failure patients. *Gadlor1/2* ablation in mice reduces cardiac hypertrophy and
5 fibrosis, and increases angiogenesis, but slows calcium re-uptake into the SR and might thereby
6 trigger arrhythmia and sudden death. Inhibition in endothelial cells and fibroblasts, on the other
7 hand, could be beneficial by increasing angiogenesis and reducing fibrosis.

Introduction

Despite recent advances in therapeutic options, chronic heart failure is still one of the leading causes of global mortality, in part due to insufficient means to counteract maladaptive cardiac remodeling.[1-3] Cardiac remodelling comprises global changes in heart shape, reduced function and arrhythmia that are the consequence of cardiomyocyte hypertrophy, altered angiogenesis and myocardial fibrosis.[4,5,6,7] The majority of current therapeutic options target protein-coding genes; however, recent studies revealed the significance of non-coding transcripts in cardiovascular development and disease conditions.[5,8,9]

Long non-coding RNAs (lncRNAs) are a diverse group of non-coding transcripts that are longer than 200 nucleotides, and that in general do not encode for proteins.[10] Due to their complex structure, lncRNAs can act, for instance, as chromatin modifiers, promote or inhibit protein-protein interactions and thereby affect protein functions, or alter mRNA stability or processing.[5] Thereby lncRNAs typically affect gene expression, alternative splicing or signalling pathways.[11,12] Recent studies have identified several lncRNAs with crucial roles in cardiac remodelling and heart failure.[11,13-16] Since non-coding transcripts are detectable in human body fluids such as in serum, circulating miRNAs and lncRNAs are currently being investigated as clinical biomarkers, as well as for being paracrine mediators of cellular communication during stress conditions.[17-19] Intra-myocardial communication is a highly regulated process governing the complex physiology of the heart, whereby proper synchronization is required between cardiomyocytes, endothelial cells (EC) and fibroblasts as the major cardiac cell types.[20,21] Cellular communication during pathological remodelling can be mediated by proteins, but also by the secretion and transfer of nanoscale extracellular vesicles (microvesicles and exosomes, termed small extracellular vesicles,

EVs, in here) that carry non-coding RNAs and alter the behaviour of recipient cells.[22-25,26,27] It is currently emerging that EVs transport lncRNAs between cells and thereby affect endothelial cell function and cardiac fibrosis, but more work is needed.[23,25,28]

Here, we studied two related and secreted lncRNAs *Gadlor1* and *Gadlor2* (GATA-downregulated long non-coding RNA), which are markedly upregulated after endothelial deletion of GATA2.[29] We found that the expression of *Gadlor* lncRNAs are significantly increased in mice after transverse aortic constriction (TAC), but also in the myocardium and serum of patients suffering from chronic heart failure. Moreover, our results revealed that *Gadlor1* and *Gadlor2* are secreted within EVs predominantly by cardiac EC, from which they are mainly taken up by cardiomyocytes, although they also have autocrine/intracrine effects on EC and fibroblasts. In cardiomyocytes, *Gadlor1/2* impact calcium handling and gene expression, while they trigger pro-fibrotic gene expression in fibroblasts and anti-angiogenic effects in EC. Our study reveals that secreted *Gadlor* lncRNAs exhibit heterocellular effects aggravating cardiac remodelling, and that targeted *Gadlor1/2* inhibition in non-myocytes might serve as a novel therapeutic strategy in heart failure.

Methods

Detailed description of materials and methods are provided in the **Supplementary Material.**

Human Samples

Studies on human heart tissue samples were approved by the Institutional Ethical Board of Massachusetts General Hospital (US), where samples were collected from patients with end-stage heart failure undergoing cardiac transplantation. Control heart tissue samples was obtained from

healthy organ donors when the organ was not eligible for transplantation, or from the victims of traffic accidents. Human serum samples were obtained from healthy blood donors, or from aortic stenosis patients before replacement of the aortic valve, where all donors provided a written informed consent for the collection and use of samples, that had received approval from Institutional Review Board of Christian-Albrechts-Universität Kiel (File number: A174/09).

Animal Models and Studies

All studies including the use and care of animals were performed with the permission of the Regional Council Karlsruhe and the Lower Saxony State Office for Consumer Protection and Food Safety, Germany. For details, see **Supplementary Material.**

Results

Increased expression of *Gadlor* lncRNAs in cardiac pressure overload in mice and in human failing hearts

Previous observations by our group had identified two previously unknown lncRNAs *Gadlor1* and *Gadlor2*, which were markedly upregulated in EC of endothelial specific GATA2 knock-out mice.[29] *Gadlor1* (AK037972) and *Gadlor2* (AK038629) are located in close proximity to each other on mouse chromosome 16, and are embedded after exon1 of the *Lsamp* (limbic system-associated membrane protein) gene in its intronic region **(Figure 1A)**. *Lsamp* is mainly expressed in the brain, and we did not detect significant *Lsamp* expression in the heart or cardiac ECs, and *Lsamp* expression patterns did not change in response to *Gadlor* knock-out in multiple organs **(Supp.**

Figure 1A-C). *Gadlor1* and *Gadlor2* fragments are not matched with any known mouse peptides (BlastP, The National Center for Biotechnology Information (NCBI) database), and we verified that they are non-coding transcripts by using the CPAT algorithm to assess protein-coding probability **(Supp. Figure 1D)**. Cardiac *Gadlor1/2* expression is low in the direct postnatal period, but becomes upregulated in the adult (2 months old) heart **(Figure 1B)**. Cellular expression analysis among the main cell types in the heart revealed the highest *Gadlor1* and *Gadlor2* expression in EC, followed by fibroblasts (FB), while the lowest levels were detected in cardiomyocytes (CM) **(Figure 1C)**. In this analysis, *Gadlor* lncRNA levels were also significantly enriched in EC versus whole heart tissue.

Next, we assessed *Gadlor1/2* RNA levels in cardiac disease. Myocardial *Gadlor1/2* expression was markedly upregulated in the chronic phase (12 weeks) after TAC versus sham **(Figure 1D)**. Predominant endothelial expression and the increased abundance during pressure overload was confirmed by fluorescent in situ hybridization **(Supp. Figure 1E-F)**.

The conservation of *Gadlor1/2* RNA between different species was analysed with the EMBOSS-Water platform by assessing the local alignment of human and mouse sequences **(Supp. Figure 2)**. *Gadlor* lncRNAs are highly conserved between human, mouse and rat. Importantly, *GADLOR1/2* expression was also strongly induced in the myocardium of patients suffering from advanced heart failure **(Figure 1E)**, and *GADLOR2* was significantly elevated in serum of patients with heart failure due to aortic stenosis **(Figure 1F)**. In this patient cohort, high *GADLOR2* levels were found mainly in patients with low left ventricular ejection fraction, and a negative correlation between these two parameters was identified **(Figure 1G).** Taken together, these results demonstrate *Gadlor1* and *Gadlor2* as lncRNAs that are co-upregulated in diseased mouse and human hearts.

1

2 ***Gadlor* lncRNAs are enriched in EC-derived extracellular vesicles (EVs)**

3 Since *GADLOR2* was detectable in serum of heart failure patients, and secreted EVs can contain
4 lncRNAs,[23,26] we hypothesized that *Gadlor*1/2 might be secreted within EVs. To test our
5 hypothesis, the abundance of *Gadlor1/2* was analysed in cultured primary mouse cardiac ECs and
6 EVs collected and purified from the supernatant of the ECs by ultracentrifugation **(Supp. Figure**
7 **3A)**. Initially, we characterized the isolated EVs with electron microscopy (EM), nanoparticle
8 tracking analysis (NTA) and FACS. We found typical microvesicles and exosomes in EM, and the
9 average size of the particles was slightly larger than 100 nm in diameter by NTA, which showed
10 that they were in the range of microvesicles and exosomes (together called as EVs in this study)
11 **(Supp. Figure 3B-C)**. Flow cytometry assessment also confirmed the presence of CD63, CD9 and
12 CD54 as common cell surface markers for EVs **(Supp. Figure 3D)**.

13 Interestingly, the absolute concentration of *Gadlor1/2* was markedly higher in cardiac EC derived
14 EVs compared to cardiac ECs themselves **(Figure 1H)**. EV *Gadlor1* and *2* RNA levels were not
15 affected by proteinase K (PK), or by RNase A, which indicated *Gadlor1/2* were encapsulated within
16 vesicles and protected from enzyme degradation **(Figure 1I)**. Indeed, *Gadlor* lncRNAs were not
17 protected upon direct incubation with PK and RNase A, or when EVs were dissolved by Triton-X,
18 before RNase A was applied **(Figure 1I)**. In addition to primary cardiac EC, also C166 mouse EC
19 secrete *Gadlor* RNAs in EVs **(Supp. Figure 3E)**. Altogether, these results suggest that *Gadlor1* and
20 *Gadlor2* are highly enriched and encapsulated in EC derived EVs.

21

1 ***Gadlor*-KO mice are protected from cardiac dysfunction during cardiac pressure-overload**

2 To investigate the role of *Gadlor* lncRNAs, systemic *Gadlor* knock-out mice (*Gadlor*-KO) were
3 generated by deletion of the whole region of mouse chromosome 16 by using a CRISPR-Cas9
4 based strategy **(Figure 1A, Figure 2A)**. Unchallenged *Gadlor*-KO mice were indistinguishable from
5 their wild-type littermates (WT) based on appearance, body weight, heart weight, and baseline
6 echocardiographic analysis **(Supp. Figure 4A-D)**. We detected, however, a mild increase in liver
7 and decrease in brain weight in KO animals compared to WT littermates (**Supp. Figure 4E**).

8 The ablation of *Gadlor1/2* was confirmed in knock-out animals by qRT-PCR in different organs
9 **(Figure 2B).** We found the highest expression levels of *Gadlor1* and *Gadlor2* in the brain, liver,
10 kidney and as well as in the heart compared to other organs in WT animals **(Figure 2B)**. To study
11 the effect of *Gadlor1* and *Gadlor2* in cardiac remodelling during pressure-overload, WT and
12 *Gadlor*-KO animals were subjected to TAC or sham surgery and subsequently monitored for 2
13 weeks **(Figure 2C)**. The carotid flow was measured after 2 days of TAC in the right and left common
14 carotid arteries to evaluate the strength of the aortic constriction. The RCCA/LCCA (right to left
15 common carotid) artery flow ratio increased to a similar degree in both WT and *Gadlor*-KO
16 animals, indicating comparable pressure overload **(Supp. Figure 4F-G).** We found a significant
17 increase in heart weight to body weight (HW/BW) ratio after 2 weeks of TAC in both WT and
18 *Gadlor*-KO compared to sham animals, however, less hypertrophy (i.e. a reduced HW/BW ratio)
19 was observed in *Gadlor*-KO mice **(Figure 2D)**. Additionally, heart-failure induced pulmonary
20 congestion was only observed in WT animals after TAC, whereas *Gadlor*-KO animals were
21 protected **(Figure 2E)**. In echocardiography, *Gadlor*-KO mice showed less cardiac systolic

dysfunction, a markedly reduced left ventricle wall thickness (LVPW) and less chamber dilation (measured as the left end-diastolic volume, LVEDV) compared to WT mice after TAC **(Figure 2F-I)**.

Deletion of *Gadlor1* and *Gadlor2* alleviates cardiomyocyte hypertrophy and fibrosis *in vivo*

Sirius red staining revealed strongly diminished myocardial fibrosis in *Gadlor*-KO mice, which was supported by reduced cardiac *Col1a1* and *Col3a1* mRNA levels after TAC **(Figure 2J-L).** A lower expression of *Nppa, Nppb*, a lower *Myh7/Myh6* RNA ratio, and a reduced cardiomyocyte cross-sectional confirmed blunted cardiac hypertrophy in *Gadlor*-KO animals compared to WT littermates after TAC **(Figure 2M-O).** Additionally, Isolectin B4 (IB4) staining of capillaries revealed a substantial increase of capillary density in the myocardium of *Gadlor*-KO mice compared to WT animals after TAC **(Figure 2N, P).** Together, our data showed that deletion of *Gadlor*1/2 protected against cardiac hypertrophy, systolic dysfunction and myocardial fibrosis during cardiac pressure-overload.

Overexpression of *Gadlor1* and *Gadlor2* via EVs triggers cardiac dysfunction and fibrosis

In order to decipher the functional effect of increased *Gadlor1* and *Gadlor2* levels during pressure-overload, we administered control EVs and *Gadlor* enriched EVs to mouse hearts directly before TAC surgery by intra-ventricular injection (and concomitant cross-clamping of aorta and pulmonary artery distal of the coronary vessels origin). Control EVs were produced by purifying EC derived EVs from the supernatant of control adenovirus (Ad.β*gal*) infected C166 mouse EC, and *Gadlor1* and *Gadlor2* containing EVs were purified from the supernatant of Ad.*Gadlor1* and

Ad.*Gadlor2* infected C166 ECs **(Figure 3A)**. We detected significantly higher levels of myocardial *Gadlor1* and *Gadlor2* after 1 week of EV administration **(Figure 3B)**. *Gadlor*-EV treated mice exerted a marked reduction of cardiac systolic function 1 and 2 weeks after TAC, as well as increased wall thickness, but unchanged left ventricular end-diastolic dimensions (LVEDA) compared to control EV treated animals (indicated as Cohort I and II **Figure 3A-E**). Histological analyses by Sirius red staining showed exaggerated myocardial fibrosis in *Gadlor*-EV treated mice, which was confirmed by qPCR of *Col1a1* and *Col3a1* mRNA expression in the myocardium **(Figure 3G-I)**. Furthermore, increased expression of *Nppa* and *Nppb*, as well as a trend towards larger cardiomyocyte cross-sectional area verified increased hypertrophic remodelling in *Gadlor*-EV treated mice **(Figure 3I-J)**. The myocardial capillary density was not changed between experimental groups **(Figure 3L)**.

We concluded that overexpression of *Gadlor1* and *Gadlor2* via administration of endothelial derived EVs aggravated cardiac dysfunction and hypertrophy, and triggered fibrosis during cardiac pressure-overload.

Gadlor-KO mice exert increased mortality during chronic pressure-overload

Next, we studied whether the protective effects of *Gadlor1/2* ablation were maintained during persisting long-term pressure overload **(Supplement Figure 5A)**. Similar to our findings after 2 weeks of TAC, *Gadlor*-KO animals had a significantly reduced HW/BW ratio after 8-weeks TAC compared to WT littermates, an improved systolic left ventricular function with reduced posterior wall thickness, an increased capillary density, diminished cardiac hypertrophy and markedly less

fibrosis **(Supplement Figure 5B-J)**. Despite retaining better systolic function and improved remodelling features, we observed a considerably higher mortality rate in *Gadlor*-KO mice starting between two and three weeks after TAC **(Supplement Figure 5K)**. Interestingly, WT and KO animals were indistinguishable in terms of appearance, behaviour and mobility after TAC operation, and death in *Gadlor*-KO mice was unexpected and sudden in nature, possibly due to cardiac arrhythmia.

***Gadlor1* and *Gadlor2* affect gene-expression and angiogenic function in ECs**

Since ECs are the main cardiac cell-type expressing *Gadlor1/2*, and since we observed an increased capillary density in the myocardium of *Gadlor*-KO mice after 2 and 8 weeks of TAC (see above), we performed RNA sequencing from isolated WT and *Gadlor*-KO ECs after 2-weeks of TAC. The purity of EC in our MACS based isolation procedure is >90%.[30] The genome-wide transcriptome analysis via bulk RNAseq identified a total of 3355 differentially expressed (DE) genes between WT and *Gadlor*-KO, which are shown in the heatmap **(Supplement Figure 6A)**. Gene ontology analysis from DE genes and RT-qPCR revealed and confirmed an upregulation of angiogenesis, mitotic cell-cycle and respiratory electron transport and a downregulation of inflammatory response genes in *Gadlor*-KO ECs after 2-weeks TAC **(Supplement Figure 6B-D)**. In addition, myocardial staining for Ki67 as proliferation marker revealed more Ki67 positive ECs in *Gadlor*-KO mice after TAC **(Supplement Figure 6E-F)**. Overexpression of *Gadlor1* and *Gadlor2* by adenovirus in C166 mouse ECs showed reduced EC sprouting activity during FGF2 and TGFβ stimulation in comparison to Ad.β*gal* (control) infected cells **(Supplement Figure 6G-H)**. In summary, *Gadlor* lncRNAs exert anti-angiogenic properties in ECs.

1

2 **Cardiac FBs of *Gadlor*-KO mice induce less fibrosis-associated genes after TAC**

3 Based on our findings, cardiac FBs exerted the second highest *Gadlor* lncRNAs expression after EC
4 **(Figure 1C).** To study FB specific gene-expression changes upon *Gadlor* knock-out, we performed
5 bulk RNAseq from isolated cardiac FBs after 2-weeks TAC. The purity of cardiac FBs in our MACS
6 based isolation procedure is >90%.[30] Genome-wide analysis revealed total of 915 downregulated
7 and 998 upregulated genes in *Gadlor*-KO FBs compared to WT mice after TAC, which are shown
8 in a heatmap in **Figure 4A**. Amongst these, we detected a strong downregulation of mainly ECM
9 organization associated genes (confirmed by RT-qPCR: *Fgfr1, Igf1, Col1a1, Col3a1, Col6a1*) **(Figure**
10 **4B-D)**. Additionally, genes related to the regulation of angiogenesis, blood vessel and
11 endothelium development were upregulated in *Gadlor*-KO FBs, which suggested a contribution
12 of FBs for vessel development and angiogenesis observed in *Gadlor*-KO ECs upon overload. The
13 increased expression of *Angpt2, Efna1, Aurkb, Dll1* in cardiac FBs from *Gadlor KO* mice was
14 confirmed by RT-qPCR **(Figure 4C)**. Upon adenoviral overexpression of *Gadlor1* and *Gadlor2*
15 followed with phenylephrine (PE) stimulation, neonatal rat cardiac fibroblasts (NRFB) exerted a
16 decreased expression of *Angpt2*, and an increased expression of *Col1a1* and *Col3a1*, but no
17 differential expression was observed for *Col4a1* or *Col6a1* **(Figure 4E)**. We concluded that *Gadlor*
18 lncRNAs trigger a pro-fibrotic gene-expression in cardiac FBs.

19

20 ***Gadlor* lncRNAs are transferred to cardiomyocytes via EC-derived EVs**

Since *Gadlor1/2* were mainly secreted by ECs, we reasoned that these lncRNAs might exert paracrine effects due to EV-mediated transfer into cardiomyocytes, where they could affect contraction, arrhythmia or hypertrophy. To analyse whether *Gadlor*1/2 are transferred from ECs to cardiomyocytes, we initially overexpressed *Gadlor1/2* by adenovirus in C166 mouse ECs, and purified EVs from the supernatant of these cells **(Figure 5A)**. We confirmed the enhancement of *Gadlor1/2* expression in EVs upon *Gadlor1/2* overexpression versus control ECs **(Figure 5B)**. The collected EVs were transferred either to neonatal rat cardiomyocytes (NRCMs) or fibroblasts (NRFBs). RT-qPCR analysis showed a significantly higher abundance of *Gadlor1/2* in NRCMs incubated with *Gadlor*-EVs compared to samples incubated with control-EVs or cardiomyocytes without any EV treatment, which indicated that EVs were taken up by CMs **(Figure 5C)**. *Gadlor* lncRNAs were also transferred from ECs to cardiomyocytes by control EVs, since higher cardiomyocyte *Gadlor1/2* levels were observed after control EV compared to non-EV treatment. Additionally, a mild increase in both *Gadlor1* and *Gadlor2* abundance was also observed in NRFBs after incubation with *Gadlor* EVs, however, at a much lower degree compared to NRCM **(Figure 5C)**. We visualized the uptake of the fluorescently-labelled (PKH67) EVs into recipient cardiomyocytes, which was analysed with confocal microscopy after 6 hours and 24 hours **(Figure 5D)**. 3D imaging by confocal Z-stacks confirmed that EVs were internalized into the recipient cardiomyocytes rather than being attached on the surface **(Supplementary Video 1)**.

Furthermore, we performed co-culture experiments with isolated *Gadlor*-KO CMs (lacking endogenous *Gadlor1/2* expression) and mouse cardiac endothelial cells (MCEC, on cell culture inserts) for 48 hours **(Figure 5E)**. *Gadlor*-KO cardiomyocytes were used to exclude confounding effects of endogenous *Gadlor1/2* expression with exogenous *Gadlor1/2* uptake from EC derived

EVs. As expected, we did not detect any *Gadlor1/2* expression in isolated *Gadlor*-KO CMs when they were kept in monoculture, whereas we detected *Gadlor1* and *Gadlor2* after co-culture with MCECs **(Figure 5F)**. These results suggested that *Gadlor1/2* were transferred into *Gadlor*-KO CMs from MCECs via EV-mediated cell-to-cell transfer. Notably, MCECs that were co-cultured with *Gadlor*-KO CMs also exerted an increase of *Gadlor1/2* expression **(Figure 5F)**, which might suggest a possible feedback mechanism between CMs and ECs.

Sub-cellular fractionation studies to localize *Gadlor* lncRNAs following EV-mediated transfer showed that *Gadlor1* and *Gadlor2* were detected in the cytosol and in a bit higher levels in the nucleus of recipient cardiomyocytes **(Figure 5G)**. Overall, endothelial-derived *Gadlor1/2* containing EVs are mainly taken up by cardiomyocytes, where they might act in the cytosol as well as in the nucleus. Cardiac FBs may mainly rely on their own cellular *Gadlor1/2* expression.

Gadlor lncRNAs bind to calcium/calmodulin-dependent protein kinase type II in cardiomyocytes

LncRNAs can interact with proteins to affect their regulatory functions.[31] Even though CMs showed the least endogenous levels of *Gadlor* lncRNAs, we still observed strong effects in cardiomyocytes (e.g. reduced hypertrophy) after *Gadlor1/2* deletion upon pressure overload. To decipher this further, we aimed at identifying the binding partners of *Gadlor1/2* in cardiomyocytes by performing RNA antisense purification coupled with mass-spectrometry (RAP-MS) in HL1 cardiac muscle cells after overexpression of *Gadlor1/2* **(Figure 6A)**. Interestingly, we found calcium/calmodulin-dependent protein kinase type II, delta (CaMKIIδ) as significant binding partner of *Gadlor1/2* **(Figure 6B)**. Next, we validated the interaction between CaMKII and

Gadlor1/2 with native RNA immunoprecipitation (RIP) followed by qRT-PCR **(Figure 6C)**. Moreover, we also identified reduced and increased phospholamban phosphorylation at the Threonine-17 (Thr17) direct CaMKII phosphorylation site in *Gadlor*-KO mice or *Gadlor*-EV treated mice after TAC, respectively **(Figure 6D-G)**. This indicated that *Gadlor1/2* might promote CaMKII activation in cardiomyocytes.

Since *Gadlor* lncRNAs had interfered in cardiac function, and CaMKII was identified as binding partner, which has a known role in cardiomyocyte excitation-contraction coupling, we investigated cardiomyocyte contractility and calcium dynamics with the Multicell HT system (Ionoptix) in isolated adult cardiomyocytes after 1-week of TAC. Interestingly, the recording software detected a considerably higher number of *Gadlor*-KO cardiomyocytes with arrhythmic behaviour during the measurements compared to WT CMs **(Figure 6H)**. Additionally, while sarcomere shortening and its timing were not affected, cardiomyocyte relaxation was delayed **(Figure 6I)**. Accordingly, *Gadlor*-KO CMs displayed a much slower re-uptake of calcium into the sarcoplasmic reticulum (SR), which led to prolonged calcium transients and also an increased calcium peak height in *Gadlor*-KO cardiomyocytes **(Figure 6J-K).** Treatment of adult mouse cardiomyocytes with *Gadlor1/2* enriched versus control EC-derived EVs led to augmented, but slower sarcomere shortening, and especially faster cardiomyocyte relaxation **(Figure 6L)**. While calcium peak height and release time were not changed, a faster diastolic calcium re-uptake was detected by a decreased tau value **(Figure 6M)**. Collectively, *Gadlor*-KO myocytes exerted enhanced arrhythmic beating, slower diastolic relaxation and calcium re-uptake into SR, which entailed increased intercellular calcium levels. Overexpression of *Gadlors1/2,* in turn, led to faster cardiomyocyte relaxation and faster re-uptake of calcium into the SR. These effects were partially

rescued upon KN93 (CaMKII inhibitor) treatment **(Supplement Figure 7)**, indicating that they might depend on *Gadlor*1/2 mediated CaMKII activation.

Gadlor1 **and** ***Gadlor2*** **affect cardiomyocyte gene expression**

Since *Gadlor1/2* were in part localized in the cardiomyocyte nucleus after transfer **(Figure 5G)**, we hypothesized that they might also affect gene expression in these cells. Comprehensive transcriptome analysis after 2-weeks TAC between isolated WT and *Gadlor*-KO cardiomyocytes revealed that 2492 genes were up-, while 2956 were downregulated after ablation of *Gadlor1/2* as shown in the heatmap in **Figure 7A**. Functional annotation of DE genes showed that genes related to vasculature development, ECM organization and regulation of cytokine production were upregulated **(Figure 7B)**, while mitochondrial organization, TCA cycle and cardiac muscle contraction genes were downregulated in *Gadlor*-KO cardiomyocytes **(Figure 7B)**. We confirmed the upregulation of *Il6, Tlr9, Col15a1, Col14a1, Adam8* RNAs, and the downregulation of *Camk2d, Gata4, Actn2, Mfn2* RNAs in Gadlor-KO cardiomyocytes after TAC by RT-qPCR **(Figure 7C-D)**. To rule out a reduced number of mitochondria as reason for the downregulation of mitochondrial genes, we assessed the mitochondrial to nuclear DNA ratio, but detected no changes in *Gadlor*-KO versus WT mice **(Figure 7E)**. We next assessed the effects of *Gadlor1/2* overexpression in cardiomyocytes after PE stimulation. **(Figure 7F)**. This showed that *Gadlor1/2* overexpression in large parts revealed the opposite effects of what was found in *Gadlor*-KO cardiomyocytes, and these effects were partially reversed upon treatment with KN93, indicating CaMKII dependent effects of *Gadlor1/2* on gene expression.

Comparing the effects of *Gadlor* knock-out in the different cardiac cell types after TAC, revealed a strong overlap among upregulated and downregulated genes in FBs, ECs and cardiomyocytes **(Supplemental Figure 8)**. For example, *Gadlor* knock-out led to the upregulation of energy coupled proton transport mitochondrial genes, actin filament associated genes, and mitotic cell cycle related genes in all three cell types, in addition the upregulation of cardiac muscle contraction and blood vessel morphogenesis genes in two cell types. On the other hand, genes related to the negative regulation of cell differentiation, cartilage development and the regulation of membrane potential were downregulated in all three cell types, while genes related to cell migration, to inflammation, to extracellular matrix organization, to heart contraction, to calcineurin/NFAT signalling and to mitochondrial organization were downregulated in at least two of the cell types **(Supplemental Figure 8)**. Therefore, *Gadlor1/2* effects on gene-expression contain common, but also unique targets in different cardiac cell types.

Discussion

Here, we describe two novel lncRNAs (termed *Gadlor1* and *Gadlor2*) as central regulators of cardiac failure during pressure overload. *Gadlor1* and *Gadlor2* were upregulated in mouse and human failing hearts as well as in serum of patients with aortic stenosis, where high *GADLOR2* levels were associated with a low ejection fraction. Accordingly, enhanced experimental *Gadlor1/2* expression in mouse hearts triggered aggravated heart failure, myocardial hypertrophy and fibrosis, while combined *Gadlor*-KO mice were protected from cardiac dysfunction, fibrosis and vascular rarefaction during acute and persisting pressure overload. Paradoxically, despite retaining better heart function and remodelling features, the complete lack of *Gadlor* lncRNAs

during chronic, persisting pressure overload entailed sudden death, most likely due to arrhythmia.

Among the different cell types in the myocardium, we found the highest *Gadlor1/2* expression in ECs, where reduced *Gadlor1/2* levels entailed an increased capillary density and increased endothelial cell proliferation after TAC. *Gadlor1/2* overexpression in isolated ECs, in turn, reduced angiogenic activity, indicating that *Gadlor* lncRNAs inhibits angiogenic activity in EC in a cell autonomous manner. Because lncRNAs often exert their effects by modifying gene-expression, we performed transcription profiling by RNA sequencing in cardiac EC after TAC. Indeed, we found that upon *Gadlor*1/2 deletion, EC upregulate genes related to angiogenesis, cell cycle and mitosis. Beside this cell autonomous role, *Gadlor*-KO mice also exerted an increased expression of proangiogenic genes in cardiomyocytes and FBs during TAC, which are known to affect angiogenesis in a paracrine manner.[32-35]

In addition to EC, cardiac FB exerted a rather high *Gadlor1/2* expression in the heart, while expression was low in cardiomyocytes. Transcriptomic profiling in cardiac FBs revealed the downregulation of many extracellular matrix-organizing genes, including pro-fibrotic growth factors, their receptors as well as matrix proteins themselves. Combined adenoviral overexpression of *Gadlor1* and *Gadlor2* in isolated rat cardiac FBs upon phenylephrine stimulation triggered the opposite effect (i.e. upregulation of matrix genes) for some, but not all of the genes identified by RNA-seq. These data imply that the pro-fibrotic role of *Gadlor1* and *Gadlor2* are mediated by their direct effect on gene-expression in cardiac FBs.

Remarkably, *Gadlor1/2* are mainly secreted within EVs from EC, which was indicated by a highly enriched *Gadlor* expression in endothelial derived EVs versus EC. This finding indicated a potential

paracrine role of *Gadlor* lncRNAs in the heart. Indeed, EVs were reported to contain mainly miRNAs, but also lncRNAs and mRNAs and to protect these RNA species from degradation by extracellular RNases.[36] EVs might thereby play a role in intercellular communication, especially during stress stimulation or disease, when their production is typically upregulated.[37] In cell culture experiments, we found an effective uptake of *Gadlor1/2* from endothelial derived EVs in neonatal and adult cardiomyocytes. When adult cardiomyocytes from *Gadlor*-KO mice that naturally could not upregulate intrinsic *Gadlor1/2* lncRNA expression were co-cultured in the bottom well of a two-chamber system with wild-type EC in the upper well, these effectively restored *Gadlor1/2* levels in the knock-out cardiomyocytes. In addition, the co-cultured EC markedly upregulated their *Gadlor1/2* expression compared to when they were cultured alone. Although we cannot prove this yet in vivo in the heart, our results nevertheless indicated a reciprocal intercellular signalling circuit between EC and cardiomyocytes, whereby EC provide *Gadlor* lncRNAs within EVs to cardiomyocytes, which signal back to EC by currently unknown mechanisms to indicate insufficient *Gadlor1/2* levels, when necessary. Indeed, signal responsive EV release had been previously described.[37]

In cardiomyocytes, *Gadlor1/2* lncRNAs are taken up from ECs localize to the cytosolic as well as to the nuclear compartment. Accordingly, we identified CaMKII as *Gadlor*1/2 binding partner in cardiomyocytes, which is activated mainly by calcium/calmodulin, autophosphorylation and oxidation or S-nitrosylation.[38] Its activity is known to be about 3-fold upregulated in failing human hearts.[39] In cardiomyocytes, CaMKII promotes on one hand maladaptive features such as cardiomyocyte hypertrophy and fibrosis by phosphorylating HDAC4, leading to de-repression of MEF2-dependent, pro-hypertrophic gene-expression.[40,41] On the other hand, it has adaptive

functions, for example, it promotes calcium re-uptake into the SR by phosphorylating phospholamban at Thr17.[42-44] Because *Gadlor1/2* bind CaMKII and *Gadlor*-KO mice exerted a reduced Thr17 phosphorylation, while *Gadlor*1/2 overexpression led to enhanced Thr17 phosphorylation, we concluded that the *Gadlor* lncRNAs might promote CaMKII activation in a feed-forward loop in cardiomyocytes during pathological overload. Decreased CaMKII activity could account for the improved cardiac remodelling features that we detected in *Gadlor* knock-out mice, and, at the same time, it slows down calcium re-uptake into the SR, leading to increased cytosolic calcium levels with pro-arrhythmic activity. Indeed, upon *Gadlor1/2* overexpression, pharmacological CaMKII inhibition partially reversed pro-hypertrophic gene-expression and reversed increased calcium cycling in isolated cardiomyocytes. With regard to their dichotomous role, *Gadlor1/2* inhibition in cardiomyocytes might not be a suitable therapeutic strategy during cardiac overload, since although it would lead to inhibition of hypertrophy, there might be the danger of arrhythmia or sudden death. On the contrary, inhibition of *Gadlor1/2* in EC and FB could be beneficial, as it would entail increased angiogenesis and reduce FB mediated fibrosis, which according to our data is likely the main underlying reason for *Gadlor1/2* triggered cardiac dysfunction. Although more work is needed, we suggest that the inhibition of *Gadlor* lncRNAs in cardiac non-myocytes might be a promising strategy to treat heart failure in the future.

Author contributions

M.K designed and performed the experiments, analysed RNAseq data and wrote the first draft of the manuscript. **S.G** designed and performed the experiments, and analysed data. **N.F**, **F.A.T**, **R.W**, **S.H, S.L, G.M.D, M.S** and **R.H** performed experiments. **D.W** designed and supervised the

generation of *Gadlor*-KO mice. **N.W** maintained the mouse colonies and performed experiments. **P.-S. K., Ja.H, D.F, S.U, K.B, A.M.G** and **J.C** provided experimental support for the study. **No.F., J.B., G.D.** and **T. W.** provide crucial advice for the study and critically revised the paper. **J.H.** designed and conceptualized the study, supervised all the experiments and prepared the final draft of the manuscript. All authors read and approved the manuscript.

Acknowledgements

The authors thank the Core Facilities Pre-Clinical Models, LIMA (Live Cell Imaging Mannheim) and the transgenic mouse service TGSM at HZI for generating the knockout mice.

Funding

This study was supported by grants from SFB1366/1-A6 (J.H.) by the Deutsche Forschungsgemeinschaft.

Disclosures

The following patent has been granted: LncRNAs Gadlor1 and 2 for use in treating and preventing cardiac remodelling. US11208656 (granted 28.01.2021).

1 **Data Availability**

2 RNA sequencing data sets were deposited in National Center for Biotechnology Information's

3 (NCBI) Gene Expression Omnibus (GEO) repository with the accession number GSE213612.

References

1. Tsao CW, Aday AW, Almarzooq ZI*, et al.* Heart Disease and Stroke Statistics-2022 Update: A Report From the American Heart Association. *Circulation* 2022;**145**:e153-e639. doi: 10.1161/CIR.0000000000001052
2. Frantz S, Hundertmark MJ, Schulz-Menger J, Bengel FM, Bauersachs J. Left ventricular remodelling post-myocardial infarction: pathophysiology, imaging, and novel therapies. *Eur Heart J* 2022;**43**:2549-2561. doi: 10.1093/eurheartj/ehac223
3. Wu X, Reboll MR, Korf-Klingebiel M, Wollert KC. Angiogenesis after acute myocardial infarction. *Cardiovasc Res* 2021;**117**:1257-1273. doi: 10.1093/cvr/cvaa287
4. Frey N, Katus HA, Olson EN, Hill JA. Hypertrophy of the heart: a new therapeutic target? *Circulation* 2004;**109**:1580-1589. doi:
5. Bar C, Chatterjee S, Falcao Pires I*, et al.* Non-coding RNAs: update on mechanisms and therapeutic targets from the ESC Working Groups of Myocardial Function and Cellular Biology of the Heart. *Cardiovasc Res* 2020;**116**:1805-1819. doi: 10.1093/cvr/cvaa195
6. Hill JA, Olson EN. Cardiac plasticity. *N Engl J Med* 2008;**358**:1370-1380. doi: 10.1056/NEJMra072139
7. Heineke J, Molkentin JD. Regulation of cardiac hypertrophy by intracellular signalling pathways. *Nat Rev Mol Cell Biol* 2006;**7**:589-600. doi:
8. Huang CK, Kafert-Kasting S, Thum T. Preclinical and Clinical Development of Noncoding RNA Therapeutics for Cardiovascular Disease. *Circ Res* 2020;**126**:663-678. doi: 10.1161/CIRCRESAHA.119.315856
9. Lu D, Thum T. RNA-based diagnostic and therapeutic strategies for cardiovascular disease. *Nat Rev Cardiol* 2019;**16**:661-674. doi: 10.1038/s41569-019-0218-x
10. Wilusz JE, Sunwoo H, Spector DL. Long noncoding RNAs: functional surprises from the RNA world. *Genes Dev* 2009;**23**:1494-1504. doi: 10.1101/gad.1800909
11. Li H, Trager LE, Liu X*, et al.* lncExACT1 and DCHS2 Regulate Physiological and Pathological Cardiac Growth. *Circulation* 2022;**145**:1218-1233. doi: 10.1161/CIRCULATIONAHA.121.056850
12. Zhao Y, Riching AS, Knight WE*, et al.* Cardiomyocyte-Specific Long Noncoding RNA Regulates Alternative Splicing of the Triadin Gene in the Heart. *Circulation* 2022;**146**:699-714. doi: 10.1161/CIRCULATIONAHA.121.058017
13. Viereck J, Kumarswamy R, Foinquinos A*, et al.* Long noncoding RNA Chast promotes cardiac remodeling. *Sci Transl Med* 2016;**8**:326ra322. doi: 10.1126/scitranslmed.aaf1475
14. Han P, Li W, Lin CH*, et al.* A long noncoding RNA protects the heart from pathological hypertrophy. *Nature* 2014;**514**:102-106. doi: 10.1038/nature13596
15. Trembinski DJ, Bink DI, Theodorou K*, et al.* Aging-regulated anti-apoptotic long non-coding RNA Sarrah augments recovery from acute myocardial infarction. *Nat Commun* 2020;**11**:2039. doi: 10.1038/s41467-020-15995-2
16. Micheletti R, Plaisance I, Abraham BJ*, et al.* The long noncoding RNA Wisper controls cardiac fibrosis and remodeling. *Sci Transl Med* 2017;**9**. doi: 10.1126/scitranslmed.aai9118
17. Cheng Y, Wang X, Yang J*, et al.* A translational study of urine miRNAs in acute myocardial infarction. *J Mol Cell Cardiol* 2012;**53**:668-676. doi: 10.1016/j.yjmcc.2012.08.010
18. Kuwabara Y, Ono K, Horie T*, et al.* Increased microRNA-1 and microRNA-133a levels in serum of patients with cardiovascular disease indicate myocardial damage. *Circ Cardiovasc Genet* 2011;**4**:446-454. doi: 10.1161/CIRCGENETICS.110.958975
19. Schulte C, Barwari T, Joshi A, Zeller T, Mayr M. Noncoding RNAs versus Protein Biomarkers in Cardiovascular Disease. *Trends Mol Med* 2020;**26**:583-596. doi: 10.1016/j.molmed.2020.02.001

20. Sluijter JP, Verhage V, Deddens JC, van den Akker F, Doevendans PA. Microvesicles and exosomes for intracardiac communication. *Cardiovasc Res* 2014;**102**:302-311. doi: 10.1093/cvr/cvu022
21. Pinto AR, Ilinykh A, Ivey MJ*, et al.* Revisiting Cardiac Cellular Composition. *Circ Res* 2016;**118**:400-409. doi: 10.1161/CIRCRESAHA.115.307778
22. Uchida S, Dimmeler S. Long noncoding RNAs in cardiovascular diseases. *Circ Res* 2015;**116**:737-750. doi: 10.1161/CIRCRESAHA.116.302521
23. Kenneweg F, Bang C, Xiao K*, et al.* Long Noncoding RNA-Enriched Vesicles Secreted by Hypoxic Cardiomyocytes Drive Cardiac Fibrosis. *Mol Ther Nucleic Acids* 2019;**18**:363-374. doi: 10.1016/j.omtn.2019.09.003
24. Piccoli MT, Gupta SK, Viereck J*, et al.* Inhibition of the Cardiac Fibroblast-Enriched lncRNA Meg3 Prevents Cardiac Fibrosis and Diastolic Dysfunction. *Circ Res* 2017;**121**:575-583. doi: 10.1161/CIRCRESAHA.117.310624
25. Hosen MR, Li Q, Liu Y*, et al.* CAD increases the long noncoding RNA PUNISHER in small extracellular vesicles and regulates endothelial cell function via vesicular shuttling. *Mol Ther Nucleic Acids* 2021;**25**:388-405. doi: 10.1016/j.omtn.2021.05.023
26. Bang C, Batkai S, Dangwal S*, et al.* Cardiac fibroblast-derived microRNA passenger strand-enriched exosomes mediate cardiomyocyte hypertrophy. *J Clin Invest* 2014;**124**:2136-2146. doi: 10.1172/JCI70577
27. Hosen MR, Goody PR, Zietzer A*, et al.* Circulating MicroRNA-122-5p Is Associated With a Lack of Improvement in Left Ventricular Function After Transcatheter Aortic Valve Replacement and Regulates Viability of Cardiomyocytes Through Extracellular Vesicles. *Circulation* 2022:101161CIRCULATIONAHA122060258. doi: 10.1161/CIRCULATIONAHA.122.060258
28. Huang G, Garikipati VNS, Zhou Y*, et al.* Identification and Comparison of Hyperglycemia-Induced Extracellular Vesicle Transcriptome in Different Mouse Stem Cells. *Cells* 2020;**9**. doi: 10.3390/cells9092098
29. Froese N, Szaroszyk M, Korf-Klingebiel M*, et al.* Endothelial Cell GATA2 Modulates the Cardiomyocyte Stress Response through the Regulation of Two Long Non-Coding RNAs. *Biology* 2022;**11**:1736. doi:
30. Froese N, Cordero J, Abouissa A*, et al.* Analysis of myocardial cellular gene expression during pressure overload reveals matrix based functional intercellular communication. *iScience* 2022;**25**:103965. doi: 10.1016/j.isci.2022.103965
31. Das S, Shah R, Dimmeler S*, et al.* Noncoding RNAs in Cardiovascular Disease: Current Knowledge, Tools and Technologies for Investigation, and Future Directions: A Scientific Statement From the American Heart Association. *Circ Genom Precis Med* 2020;**13**:e000062. doi: 10.1161/HCG.0000000000000062
32. Heineke J, Auger-Messier M, Xu J*, et al.* Cardiomyocyte GATA4 functions as a stress-responsive regulator of angiogenesis in the murine heart. *J Clin Invest* 2007;**117**:3198-3210. doi: 10.1172/JCI32573
33. Dittrich GM, Froese N, Wang X*, et al.* Fibroblast GATA-4 and GATA-6 promote myocardial adaptation to pressure overload by enhancing cardiac angiogenesis. *Basic Res Cardiol* 2021;**116**:26. doi: 10.1007/s00395-021-00862-y
34. Sano M, Minamino T, Toko H*, et al.* p53-induced inhibition of Hif-1 causes cardiac dysfunction during pressure overload. *Nature* 2007;**446**:444-448. doi:
35. Vidal R, Wagner JUG, Braeuning C*, et al.* Transcriptional heterogeneity of fibroblasts is a hallmark of the aging heart. *JCI Insight* 2019;**4**. doi: 10.1172/jci.insight.131092
36. Kim KM, Abdelmohsen K, Mustapic M, Kapogiannis D, Gorospe M. RNA in extracellular vesicles. *Wiley Interdiscip Rev RNA* 2017;**8**. doi: 10.1002/wrna.1413
37. Pironti G, Strachan RT, Abraham D*, et al.* Circulating Exosomes Induced by Cardiac Pressure Overload Contain Functional Angiotensin II Type 1 Receptors. *Circulation* 2015;**131**:2120-2130. doi: 10.1161/CIRCULATIONAHA.115.015687

38. Mattiazzi A, Bassani RA, Escobar AL*, et al.* Chasing cardiac physiology and pathology down the CaMKII cascade. *Am J Physiol Heart Circ Physiol* 2015;**308**:H1177-1191. doi: 10.1152/ajpheart.00007.2015
39. Kirchhefer U, Schmitz W, Scholz H, Neumann J. Activity of cAMP-dependent protein kinase and Ca2+/calmodulin-dependent protein kinase in failing and nonfailing human hearts. *Cardiovasc Res* 1999;**42**:254-261. doi: 10.1016/s0008-6363(98)00296-x
40. Backs J, Backs T, Neef S*, et al.* The delta isoform of CaM kinase II is required for pathological cardiac hypertrophy and remodeling after pressure overload. *Proc Natl Acad Sci U S A* 2009;**106**:2342-2347. doi: 0813013106 [pii]

10.1073/pnas.0813013106
41. Li C, Cai X, Sun H*, et al.* The deltaA isoform of calmodulin kinase II mediates pathological cardiac hypertrophy by interfering with the HDAC4-MEF2 signaling pathway. *Biochem Biophys Res Commun* 2011;**409**:125-130. doi: 10.1016/j.bbrc.2011.04.128
42. Beckendorf J, van den Hoogenhof MMG, Backs J. Physiological and unappreciated roles of CaMKII in the heart. *Basic Res Cardiol* 2018;**113**:29. doi: 10.1007/s00395-018-0688-8
43. Mattiazzi A, Kranias EG. The role of CaMKII regulation of phospholamban activity in heart disease. *Front Pharmacol* 2014;**5**:5. doi: 10.3389/fphar.2014.00005
44. Kemi OJ, Ellingsen O, Ceci M*, et al.* Aerobic interval training enhances cardiomyocyte contractility and Ca2+ cycling by phosphorylation of CaMKII and Thr-17 of phospholamban. *J Mol Cell Cardiol* 2007;**43**:354-361. doi: 10.1016/j.yjmcc.2007.06.013

Figure Legends

Figure 1: *Gadlor* lncRNAs are mainly expressed in cardiac endothelial cells (ECs) and their expression is highly increased in mice after pressure-overload and in human failing hearts.

A. Representative scheme of AK037972 *(Gadlor1)* and AK038629 *(Gadlor2)* locus on mouse chromosome 16 and positions of the CRISPR/ Cas9 deletion sites used to generate *Gadlor*-KO mice. **B.** *Gadlor1* and *Gadlor2* expression levels in mouse cardiac tissue from different postnatal developmental stages (P1 – n=5, P5 – n=5, P21 – n=3 and adult (9-weeks old) – n=4), and in **C.** different cardiac cell-types (EC: endothelial cells – n=5, FB: fibroblast – n=6, CM: cardiomyocytes – n=4) and heart tissue (WH: whole heart – n=6). **D.** *Gadlor* lncRNA levels in mouse cardiac tissue after long-term (12 weeks, n=9) TAC (transverse aortic constriction) compared to sham. **E.** *GADLOR1* and *2* expression in control (healthy, n=6) and human failing heart tissue (n=8) samples. **F.** Detection of *GADLOR2* levels (pg/l: picogram/liter) in human serum of healthy volunteers (n=19) and patients with aortic stenosis (n=16). **G.** Correlation analysis of *GADLOR2*

levels (pg/l) with ejection fraction (%) of the aortic stenosis patients (n=16) from **F**, (Pearson correlation, Pearson r= -4892 and p-value = 0.0272). **H.** Absolute quantification of total RNA amount of *Gadlor1* and *Gadlor2* in ECs and EC-derived EVs (fg/ng: femtogram/ nanogram). **I.** Detection of *Gadlor* lncRNAs in EC-derived EVs treated with proteinase K (PK), RNase or Triton-X as indicated. Data are shown as mean±SEM. Data normality was evaluated with the Shapiro-Wilk test. *P*-values were calculated with Student's t-test for parametric (or Mann-Whitney for non-parametric) for comparing two groups, and one-way ANOVA was applied for comparing multiple groups followed with Fisher's LSD post-hoc test. *p-value<0.05, **p-value<0.01, ***p-value<0.001, ****p-value<0.0001.

Figure 2: Deletion of *Gadlor* lncRNAs reduces cardiac hypertrophy and fibrosis during cardiac pressure overload.

A. Scheme of *Gadlor*-KO mouse line generation by systemic deletion of the region on chromosome 16 containing both *Gadlor1* and *Gadlor2* by a CRISPR/Cas9 approach. **B.** Assessment of the relative expression of *Gadlor*s in indicated organs in adult WT and *Gadlor*-KO mice (n≥8). The difference in *Gadlor1/2* expression levels between WT and *Gadlor*-KO animals were significant for all organs, in which *Gadlor1* and *Gadlor2* were detected. (Heart: *p-value<0.05, Liver and Kidney: ***p-value<0.001, Brain: ****p-value<0.0001). **C.** Experimental design of TAC operation for *Gadlor*-KO and WT littermates. **D.** Heart weight to body weight ratio (HW/BW, mg/g) and **E.** lung weight (mg) to body weight (g) ratio of *Gadlor*-KO and WT littermates in sham and after 2 weeks TAC (n≥11). **F.** Representative echocardiography images of *Gadlor*-KO and WT mice before (pre-TAC) and after 2 weeks of TAC (2w TAC) shown in parasternal long axis mode, and analysis of **G.** left ventricle (LV) ejection fraction (EF%), **H.** LV posterior wall thickness in diastole (mm) and **I.** LV end diastolic volume (ul), (n≥12). **J.** Representative Sirius-red fibrosis staining in cardiac tissue sections of sham and 2w TAC animals (scale-bar: 1 mm) and **K.** quantification of fibrotic area (n≥4). **L.** Relative mRNA expression of fibrosis marker and **M.** hypertrophy marker genes in heart tissue

samples of sham (n=3) and 2w TAC (n=5). **N.** Representative immunofluorescence images of cardiac tissue samples stained with WGA (wheat-germ agglutinin coupled with Alexa Fluor 555) and IB4 (Isolectin B4 coupled with Alexa Fluor 488) in sham and 2-week TAC samples from *Gadlor*-KO and WT littermates, scale-bar: 100 µm. Quantification of **O.** cardiomyocyte cross-sectional area and **P.** myocardial capillary density per cardiomyocyte ratio. Data are shown as mean±SEM. Data normality was evaluated with Shapiro-Wilk test and p-values were calculated with Student's t-test for comparing two groups and two-way ANOVA for grouped analysis followed with Fisher's LSD post-hoc test. *p-value<0.05, **p-value<0.01, ***p-value<0.001, ****p-value<0.0001.

Figure 3: Cardiac overexpression of *Gadlor1* and *Gadlor2* triggers cardiac dysfunction and fibrosis after TAC.

A. Scheme of the experimental design depicting the injection of *Gadlor1 and Gadlor2* containing or control extracellular vesicles (EVs) followed by TAC surgery. **B.** Relative expression of *Gadlor1 and Gadlor2* in cardiac tissue samples after 1 week TAC (cohort I) to validate the overexpression after injection of control (Ad.βgal treated samples, n=5) and *Gadlor*-containing (Ad.*Gadlor1* and Ad.*Gadlor2* treated samples, n=6) EVs. Echocardiographic analysis of **C.** left ventricle (LV) ejection fraction (EF%) after 1-week TAC, and **D.** LV-EF%, **E.** LV posterior wall thickness in diastole (mm), **F.** LV-end diastolic area (mm^2) after 2 weeks TAC in mice injected with control EVs and *Gadlor*1 and *Gadlor2* EVs (cohort II). **G.** Representative images of Sirius-red staining (scale bar: 1 mm) and **H.** quantification of fibrotic area after 2 weeks TAC in mice injected with control or *Gadlor*1 and *Gadlor2* EVs. **I.** Relative expression of indicated fibrosis and hypertrophy genes in heart tissue samples of control EV (n=6) and *Gadlor* EVs (n=6) treated mice. **J.** Representative immunofluorescence images of cardiac tissue samples stained with WGA (wheat-germ agglutinin coupled with Alexa Fluor 555) and IB4 (Isolectin B4 coupled with Alexa Fluor 488) in samples from control-EV and *Gadlor*-EV treated animals (scale-bar: 100 µm). Quantification of **K.** cardiomyocyte cross-sectional area

and **L.** myocardial capillarization after EV treatment followed by 2 weeks of TAC. Data are shown as mean±SEM. Data normality was evaluated with Shapiro-Wilk test and p-values were calculated with Student's t-test. *p-value<0.05, **p-value<0.01, ***p-value<0.001, ****p-value<0.0001.

Figure 4: RNA sequencing of *Gadlor*-KO cardiac FBs showed less induction of fibrosis-associated genes after TAC.

A. Heatmap showing differentially regulated genes analysed by bulk RNAseq of isolated cardiac fibroblasts after 2-weeks TAC. **B.** Bar plots showing the gene-ontology (GO) analysis of upregulated and downregulated genes in *Gadlor*-KO FBs after 2-weeks TAC (Red: Upregulated in *Gadlor*-KO, Blue: Downregulated in *Gadlor*-KO). Exemplary genes were listed for selected GO-terms. **C-D.** Validation of selected genes from RNAseq data with qRT-PCR in isolated adult cardiac FBs after 2 weeks of TAC (Red: Upregulated in *Gadlor*-KO, Blue: Downregulated in *Gadlor*-KO). **E.** qRT-PCR of selected genes in neonatal rat fibroblasts (NRFB) overexpressing *Gadlor* lncRNAs after *Gadlor1/2* adenovirus treatment (*βgal* as control) followed by phenylephrine (PE) stimulation (100 µM, 24 hours). Data are shown as mean±SEM. Data normality was evaluated with Shapiro-Wilk test and p-values were calculated with Student's t-test for parametric and Mann-Whitney test for non-parametric assessment. *p-value<0.05.

Figure 5: Secreted *Gadlor* lncRNAs are transferred to cardiomyocytes via endothelial-derived EVs.

A. Schematic representation of experimental design of EV (isolated from C166 endothelial cells, EC, supernatant) transfer to NRCMs or NRFBs. **B.** Validation of *Gadlor1* and *Gadlor2* overexpression in isolated EVs. **C.** RT-qPCR detection of *Gadlor1* and *Gadlor2* after transferring control EVs (isolated from Ad*βgal* treated ECs) or *Gadlor*-EVs (isolated from Ad*Gadlor1/* 2 treated ECs) on neonatal rat cardiomyocytes (NRCMs) or neonatal rat cardiac fibroblasts (NRFBs). The samples were collected after 6 hours of EV

incubation. **D.** Visualization of NRCMs that were incubated with PKH67-labelled (green) EVs isolated from C166 ECs for 6 hours and 24 hours. Staining was performed with Phalloidin (red) and DAPI (blue). Scale bar: 50 µm. **E.** Scheme of co-culture experiment with transwell (1 µm pore diameter – allows EV transfer). Mouse cardiac EC (MCEC) on top cultured with *Gadlor*-KO CMs in the bottom well without direct cell contact. **F.** RT-qPCR detection of *Gadlor1* and *Gadlor2* in isolated *Gadlor*-KO CMs and MCEC mouse ECs after 48 hours of mono-culture or co-culture as indicated. **G.** *Gadlor1* and *Gadlor2* expression in the cytosol and nucleus of the recipient NRCMs after EV transfer (as shown in A). Data are shown as mean±SEM. Data normality was evaluated with Shapiro-Wilk test. P-values were calculated with Student's t-test or one-way ANOVA with Fisher's LSD post-hoc test for comparing two or multiple groups, respectively. Two-way ANOVA with Fisher's LSD post-hoc test was applied for grouped analysis when applicable. *p-value<0.05, **p-value<0.01, ***p-value<0.001, ****p-value<0.0001.

Figure 6. *Gadlor* lncRNAs bind to calcium/calmodulin-dependent protein kinase type II in cardiomyocytes.

A. Experimental scheme of RNA-antisense purification coupled with mass spectroscopy (RAP-MS) to identify specific interaction partners of *Gadlor1/2* in HL1 cardiomyocytes treated with βgal and *Gadlor1/2* adenovirus. **B.** Volcano plot indicating the identified interaction partners of *Gadlor1* and *Gadlor2* in cardiomyocytes with RAP-MS (Fold change enrichment (FC) threshold 1.2 and p-value < 0.05). UV crosslinking was used to stabilize protein:RNA interactions and non-crosslinked (N-XL) samples were used as background and removed from crosslinked (XL) samples for each indicated condition. **C.** RNA immunoprecipitation (RIP) performed with anti-IgG or anti-CaMKII antibodies from HL-1 cardiac muscle cell lysate to validate the interaction with *Gadlors*. RT-qPCR analysis showing the enrichment of *Gadlor1* and *Gadlor2* compared to IgG controls. Data was normalized to input RNA expression. (n=3 for each condition) **D-E.** Exemplary Western blots of phospho-Thr17-PLN and total PLN with CSQ as loading control

in **(D)** WT and *Gadlor*-KO and **(E)** in control-EV and Gadlor-EV treated mouse heart tissue samples after 2 weeks TAC. **F-G.** Quantification of Western-blots. **H.** Percentage of isolated adult WT and *Gadlor-KO* cardiomyocytes with arrhythmic phenotype after 1-week TAC recorded by Multicell HT system (Ion-Optix) Cell number≥30 in each condition. Sarcomere contractility **(I-K)** and calcium transient **(L-M)** measurements were recorded in parallel with Multicell HT system with continuous perfusion of basal media on isolated adult CMs after 1-week TAC. **I.** Contractility parameters including sarcomere shortening (%) and relaxation. **J.** Calcium parameters including calcium peak height (arbitrary units, AU) and decay time (tau, seconds). **K.** Representative calcium transient recordings of WT and *Gadlor*-KO mice shown as normalized levels of calcium (%). **L.** Sarcomere function and **M.** calcium transient and decay time constant (tau). Recordings were obtained from adult cardiomyocytes isolated from WT mice after 1 week TAC followed by incubation of control-EV (Ad.βgal) and *Gadlor1/2*-EVs (Ad.Gadlor1 and Ad.Gadlor2) for 4-6 hours. Data are shown as mean±SEM. Data normality was evaluated with Shapiro-Wilk test and p-values were calculated with Student's t-test (Mann-Whitney for non-parametric) for comparing two groups. *p-value<0.05, **p-value<0.01, ***p-value<0.001, ****p-value<0.0001.

Figure 7. Deletion of *Gadlor1* and *Gadlor2* affects gene expression in cardiomyocytes.

A. Heatmap showing differentially regulated genes analysed by bulk RNAseq of isolated cardiomyocytes after 2-weeks TAC. **B.** Bar plots showing the gene-ontology (GO) analysis of upregulated and downregulated genes in *Gadlor*-KO CMs after 2-weeks TAC. (Red: Upregulated in *Gadlor*-KO, Blue: Downregulated in *Gadlor*-KO). Exemplary genes were listed for selected GO-terms. **C-D.** Validation of selected upregulated and downregulated genes from RNAseq data with qRT-PCR. **E.** Analysis of mitochondrial DNA (mtDNA) to nuclear DNA (nDNA) ratio determined via quantitative PCR by using WT and *Gadlor-KO* heart tissue samples isolated 2-weeks after TAC. Assessment of ND1 and 16S DNA abundance was used to determine the mtDNA/ nDNA ratio. **F.** qRT-PCR of selected genes in HL-1 cardiac

1 muscle cells overexpressing *Gadlor* lncRNAs after *Gadlor1/2* adenovirus treatment (*βgal* as control)
2 followed by phenylephrine (PE) stimulation (100 µM, 24 hours) with and without KN93 (1 µM, 2 hours)
3 addition. Data are shown as mean±SEM. Data normality was evaluated with Shapiro-Wilk test. P-values
4 were calculated with Student's t-test for parametric (or Mann-Whitney for non-parametric) for comparing
5 two groups. Two-way ANOVA with Fisher's LSD post-hoc test was applied for grouped analysis. ns: no
6 significance, *p-value<0.05, **p-value<0.01, ***p-value<0.001, ****p-value<0.0001.

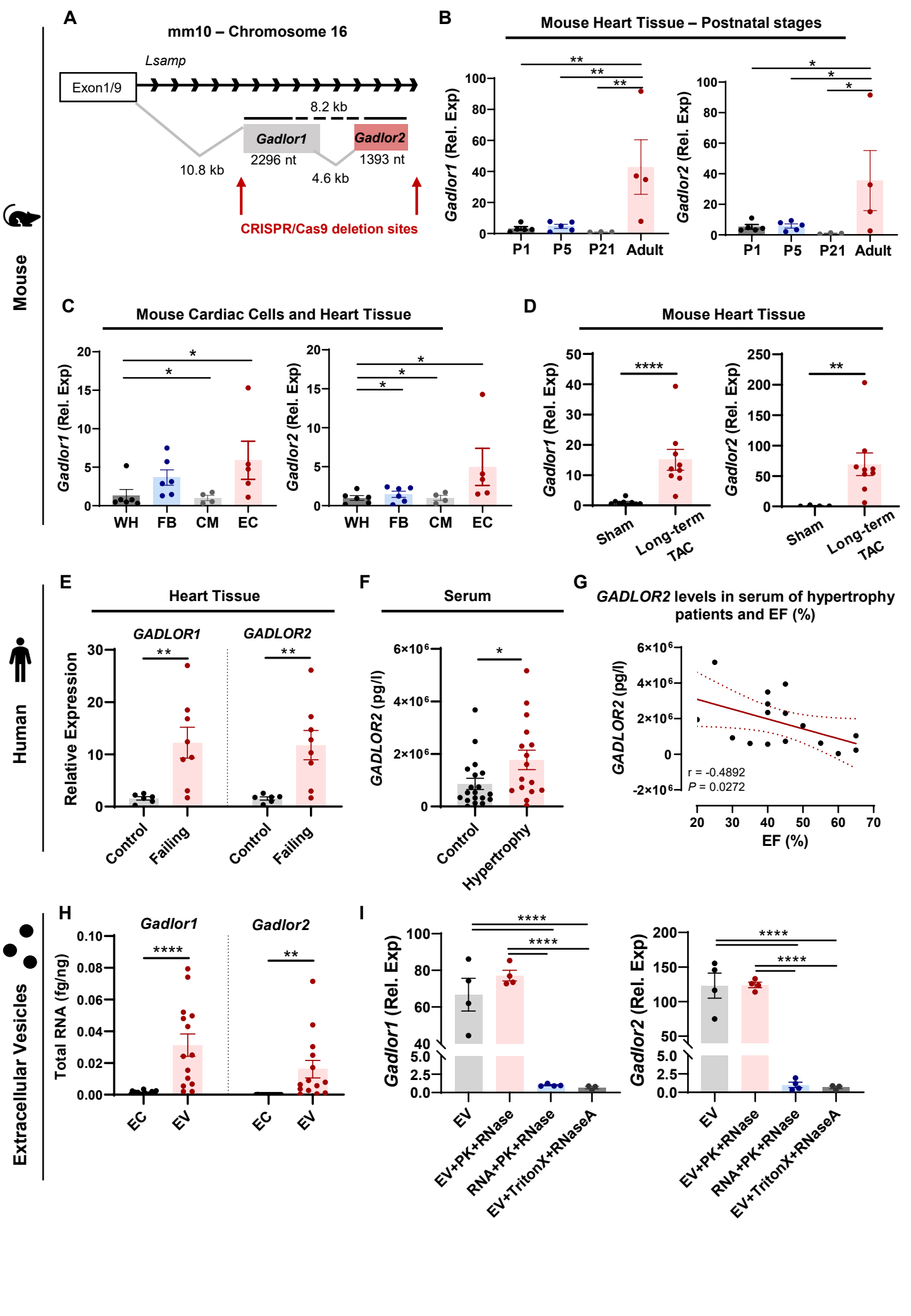
A
mm10 – Chromosome 16
Lsamp
Exon1/9
8.2 kb
Gadlor1
Gadlor2
2296 nt
1393 nt
10.8 kb
4.6 kb
CRISPR/Cas9 deletion sites
B
Mouse Heart Tissue – Postnatal stages
Gadlor1 (Rel. Exp)
Gadlor2 (Rel. Exp)
P1
P5
P21
Adult
Mouse
C
Mouse Cardiac Cells and Heart Tissue
WH
FB
CM
EC
D
Mouse Heart Tissue
Sham
Long-term TAC
Human
E
Heart Tissue
GADLOR1
GADLOR2
Relative Expression
Control
Failing
F
Serum
GADLOR2 (pg/l)
Control
Hypertrophy
G
GADLOR2 levels in serum of hypertrophy patients and EF (%)
r = -0.4892
P = 0.0272
EF (%)
Extracellular Vesicles
H
Gadlor1
Gadlor2
Total RNA (fg/ng)
EC
EV
I
EV
EV+PK+RNase
RNA+PK+RNase
EV+TritonX+RNaseA

Figure 1: *Gadlor* lncRNAs are mainly expressed in cardiac endothelial cells (ECs) and their expression is highly increased in mice after pressure-overload and in human failing hearts.

A. Representative scheme of AK037972 *(Gadlor1)* and AK038629 *(Gadlor2)* locus on mouse chromosome 16 and positions of the CRISPR/ Cas9 deletion sites used to generate *Gadlor*-KO mice. **B.** *Gadlor1* and *Gadlor2* expression levels in mouse cardiac tissue from different postnatal developmental stages (P1 – n=5, P5 – n=5, P21 – n=3 and adult (9-weeks old) – n=4), and in **C.** different cardiac cell-types (EC: endothelial cells – n=5, FB: fibroblast – n=6, CM: cardiomyocytes – n=4) and heart tissue (WH: whole heart – n=6). **D.** *Gadlor* lncRNA levels in mouse cardiac tissue after long-term (12 weeks, n=9) TAC (transverse aortic constriction) compared to sham. **E.** *GADLOR1* and *2* expression in control (healthy, n=6) and human failing heart tissue (n=8) samples. **F.** Detection of *GADLOR2* levels (pg/l: picogram/liter) in human serum of healthy volunteers (n=19) and patients with aortic stenosis (n=16). **G.** Correlation analysis of *GADLOR2* levels (pg/l) with ejection fraction (%) of the aortic stenosis patients (n=16) from **F**, (Pearson correlation, Pearson r= -4892 and p-value = 0.0272). **H.** Absolute quantification of total RNA amount of *Gadlor1* and *Gadlor2* in ECs and EC-derived EVs (fg/ng: femtogram/ nanogram). **I.** Detection of *Gadlor* lncRNAs in EC-derived EVs treated with proteinase K (PK), RNase or Triton-X as indicated. Data are shown as mean±SEM. Data normality was evaluated with the Shapiro-Wilk test. *P*-values were calculated with Student's t-test for parametric (or Mann-Whitney for non-parametric) for comparing two groups, and one-way ANOVA was applied for comparing multiple groups followed with Fisher's LSD post-hoc test. *p-value<0.05, **p-value<0.01, ***p-value<0.001, ****p-value<0.0001.

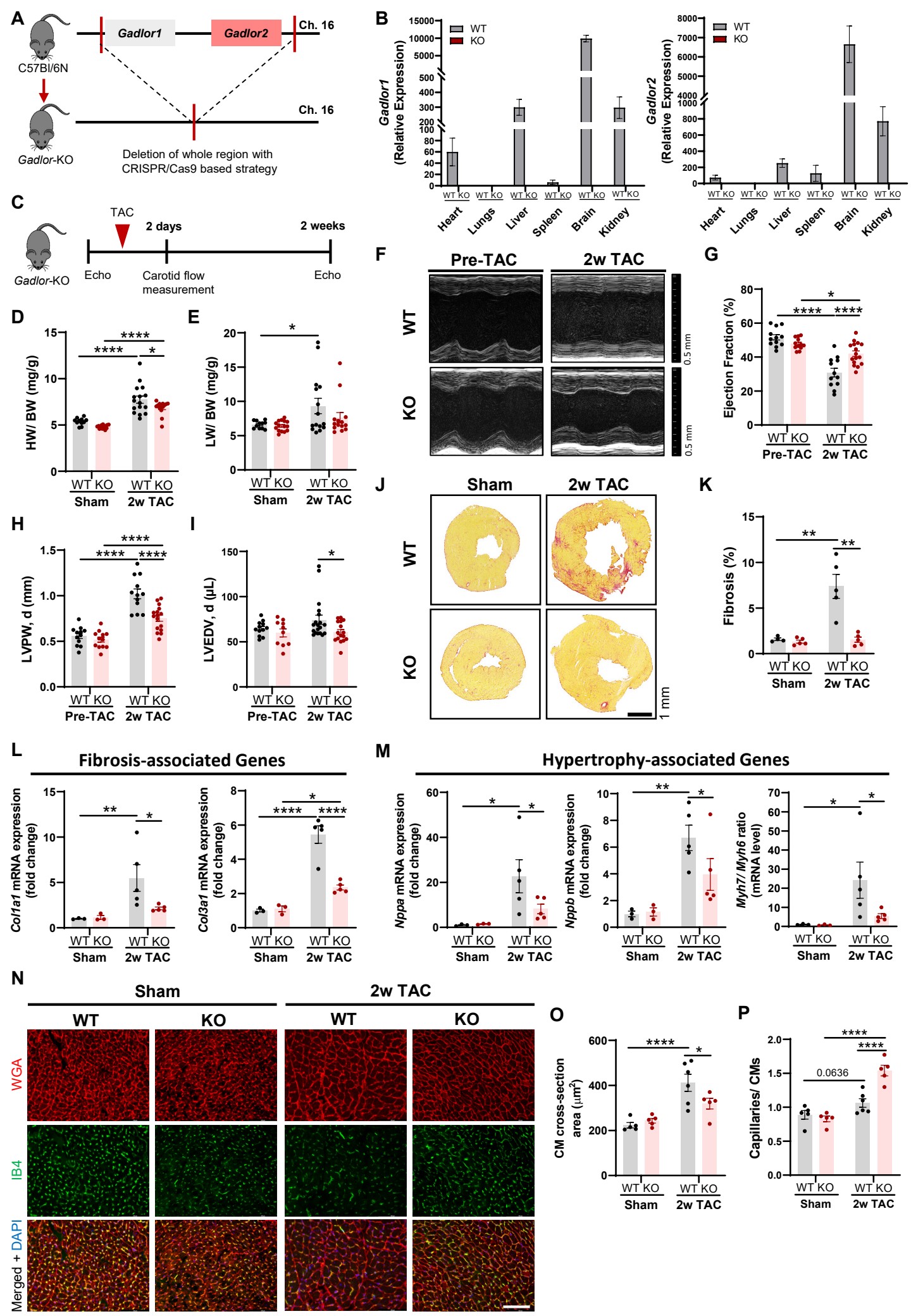
A
C57Bl/6N
Gadlor1
Gadlor2
Ch. 16
Ch. 16
Gadlor-KO
Deletion of whole region with CRISPR/Cas9 based strategy
B
WT
KO
Gadlor1 (Relative Expression)
Gadlor2 (Relative Expression)
Heart
Lungs
Liver
Spleen
Brain
Kidney
C
TAC
2 days
2 weeks
Gadlor-KO
Echo
Carotid flow measurement
Echo
D
HW/ BW (mg/g)
E
LW/ BW (mg/g)
Sham
2w TAC
F
Pre-TAC
2w TAC
WT
KO
0.5 mm
G
Ejection Fraction (%)
Pre-TAC
2w TAC
H
LVPW, d (mm)
I
LVEDV, d (µL)
J
Sham
2w TAC
1 mm
K
Fibrosis (%)
L
Fibrosis-associated Genes
Col1a1 mRNA expression (fold change)
Col3a1 mRNA expression (fold change)
M
Hypertrophy-associated Genes
Nppa mRNA expression (fold change)
Nppb mRNA expression (fold change)
Myh7/ Myh6 ratio (mRNA level)
N
Sham
2w TAC
WT
KO
WGA
IB4
Merged + DAPI
O
CM cross-section area (µm²)
P
Capillaries/ CMs
0.0636

Figure 2: Deletion of *Gadlor* lncRNAs reduces cardiac hypertrophy and fibrosis during cardiac pressure overload.

A. Scheme of *Gadlor*-KO mouse line generation by systemic deletion of the region on chromosome 16 containing both *Gadlor1* and *Gadlor2* by a CRISPR/Cas9 approach. **B.** Assessment of the relative expression of *Gadlor*s in indicated organs in adult WT and *Gadlor*-KO mice (n≥8). The difference in *Gadlor1/2* expression levels between WT and *Gadlor*-KO animals were significant for all organs, in which *Gadlor1* and *Gadlor2* were detected. (Heart: *p-value<0.05, Liver and Kidney: ***p-value<0.001, Brain: ****p-value<0.0001). **C.** Experimental design of TAC operation for *Gadlor*-KO and WT littermates. **D.** Heart weight to body weight ratio (HW/BW, mg/g) and **E.** lung weight (mg) to body weight (g) ratio of *Gadlor*-KO and WT littermates in sham and after 2 weeks TAC (n≥11). **F.** Representative echocardiography images of *Gadlor*-KO and WT mice before (pre-TAC) and after 2 weeks of TAC (2w TAC) shown in parasternal long axis mode, and analysis of **G.** left ventricle (LV) ejection fraction (EF%), **H.** LV posterior wall thickness in diastole (mm) and **I.** LV end diastolic volume (ul), (n≥12). **J.** Representative Sirius-red fibrosis staining in cardiac tissue sections of sham and 2w TAC animals (scale-bar: 1 mm) and **K.** quantification of fibrotic area (n≥4). **L.** Relative mRNA expression of fibrosis marker and **M.** hypertrophy marker genes in heart tissue samples of sham (n=3) and 2w TAC (n=5). **N.** Representative immunofluorescence images of cardiac tissue samples stained with WGA (wheat-germ agglutinin coupled with Alexa Fluor 555) and IB4 (Isolectin B4 coupled with Alexa Fluor 488) in sham and 2-week TAC samples from *Gadlor*-KO and WT littermates, scale-bar: 100 µm. Quantification of **O.** cardiomyocyte cross-sectional area and **P.** myocardial capillary density per cardiomyocyte ratio. Data are shown as mean±SEM. Data normality was evaluated with Shapiro-Wilk test and p-values were calculated with Student's t-test for comparing two groups and two-way ANOVA for grouped analysis followed with Fisher's LSD post-hoc test. *p-value<0.05, **p-value<0.01, ***p-value<0.001, ****p-value<0.0001.

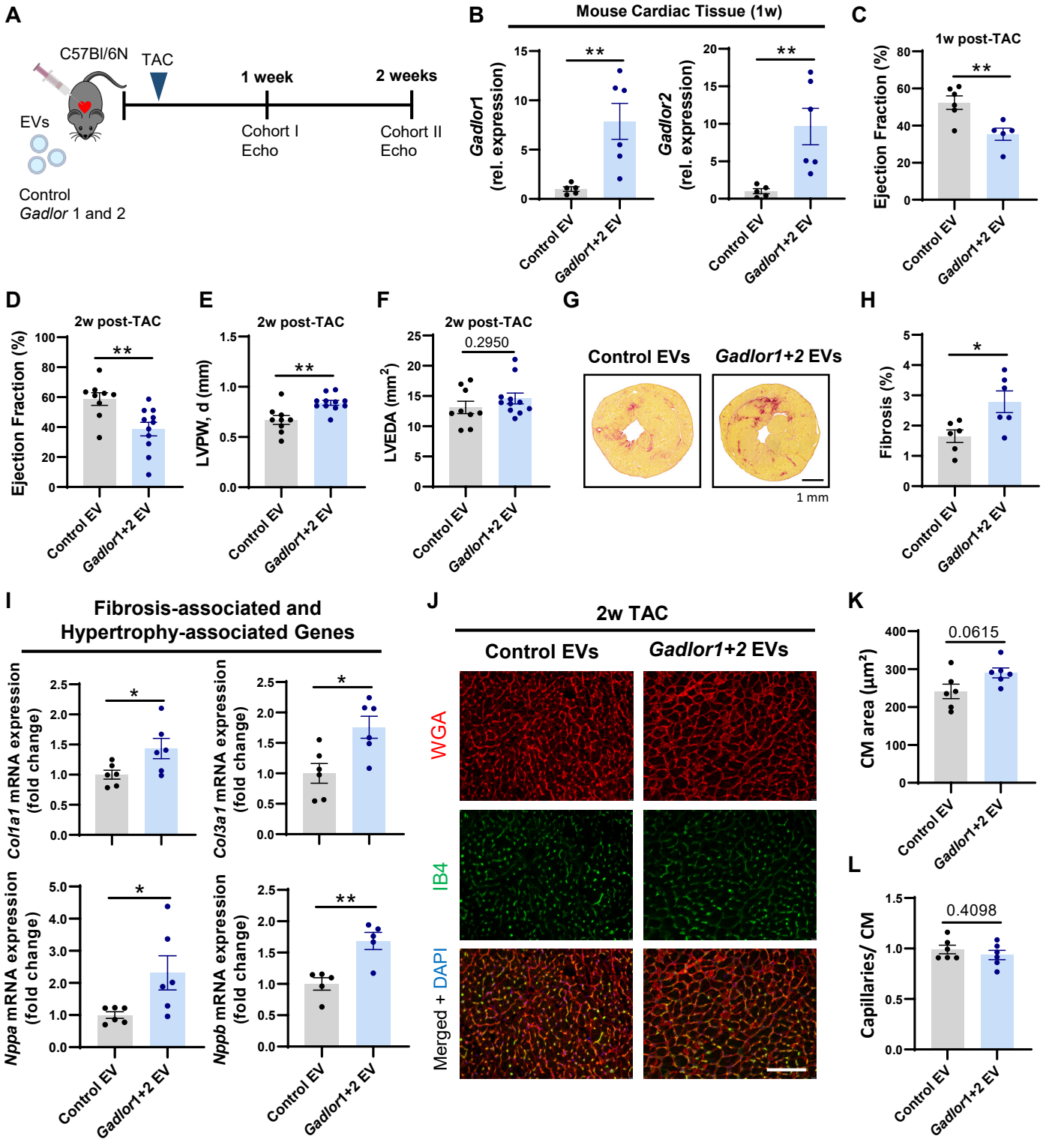

Figure 3: Cardiac overexpression of *Gadlor1* and *Gadlor2* triggers cardiac dysfunction and fibrosis after TAC.

A. Scheme of the experimental design depicting the injection of *Gadlor1 and Gadlor2* containing or control extracellular vesicles (EVs) followed by TAC surgery. **B.** Relative expression of *Gadlor1 and Gadlor2* in cardiac tissue samples after 1 week TAC (cohort I) to validate the overexpression after injection of control (Ad.βgal treated samples, n=5) and *Gadlor*-containing (Ad.*Gadlor1* and Ad.*Gadlor2* treated samples, n=6) EVs. Echocardiographic analysis of **C.** left ventricle (LV) ejection fraction (EF%) after 1-week TAC, and **D.** LV-EF%, **E.** LV posterior wall thickness in diastole (mm), **F.** LV-end diastolic area (mm^2) after 2 weeks TAC in mice injected with control EVs and *Gadlor*1 and *Gadlor2* EVs (cohort II). **G.** Representative images of Sirius-red staining (scale bar: 1 mm) and **H.** quantification of fibrotic area after 2 weeks TAC in mice injected with control or *Gadlor*1 and *Gadlor2* EVs. **I.** Relative expression of indicated fibrosis and hypertrophy genes in heart tissue samples of control EV (n=6) and *Gadlor* EVs (n=6) treated mice. **J.** Representative immunofluorescence images of cardiac tissue samples stained with WGA (wheat-germ agglutinin coupled with Alexa Fluor 555) and IB4 (Isolectin B4 coupled with Alexa Fluor 488) in samples from control-EV and *Gadlor*-EV treated animals (scale-bar: 100 µm). Quantification of **K.** cardiomyocyte cross-sectional area and **L.** myocardial capillarization after EV treatment followed by 2 weeks of TAC. Data are shown as mean±SEM. Data normality was evaluated with Shapiro-Wilk test and p-values were calculated with Student's t-test. *p-value<0.05, **p-value<0.01, ***p-value<0.001, ****p-value<0.0001.

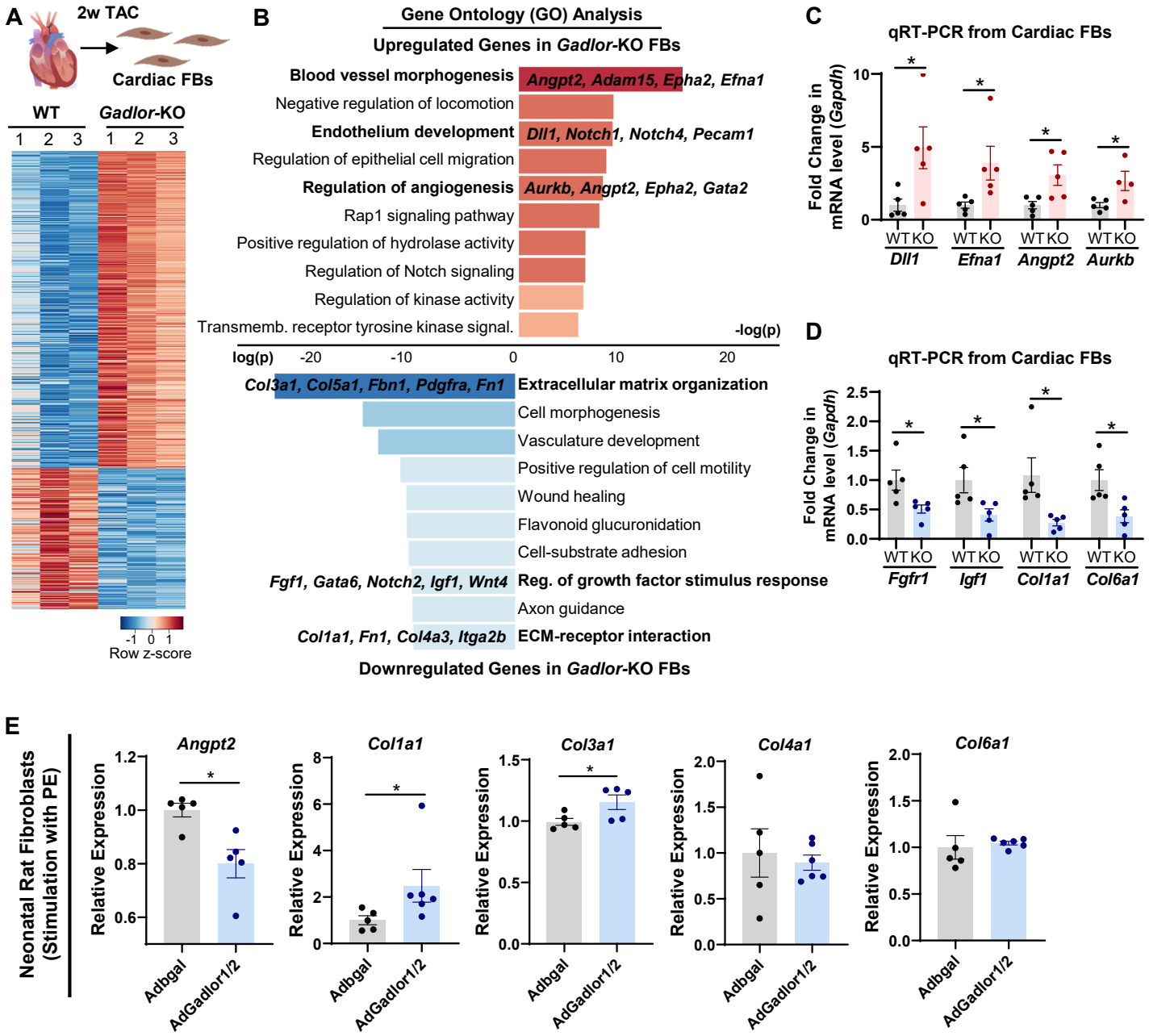

Figure 4: RNA sequencing of *Gadlor*-KO cardiac FBs showed less induction of fibrosis-associated genes after TAC.

A. Heatmap showing differentially regulated genes analysed by bulk RNAseq of isolated cardiac fibroblasts after 2-weeks TAC. **B.** Bar plots showing the gene-ontology (GO) analysis of upregulated and downregulated genes in *Gadlor*-KO FBs after 2-weeks TAC (Red: Upregulated in *Gadlor*-KO, Blue: Downregulated in *Gadlor*-KO). Exemplary genes were listed for selected GO-terms. **C-D.** Validation of selected genes from RNAseq data with qRT-PCR in isolated adult cardiac FBs after 2 weeks of TAC (Red: Upregulated in *Gadlor*-KO, Blue: Downregulated in *Gadlor*-KO). **E.** qRT-PCR of selected genes in neonatal rat fibroblasts (NRFB) overexpressing *Gadlor* lncRNAs after *Gadlor1/2* adenovirus treatment (*βgal* as control) followed by phenylephrine (PE) stimulation (100 µM, 24 hours). Data are shown as mean±SEM. Data normality was evaluated with Shapiro-Wilk test and p-values were calculated with Student's t-test for parametric and Mann-Whitney test for non-parametric assessment. *p-value<0.05.

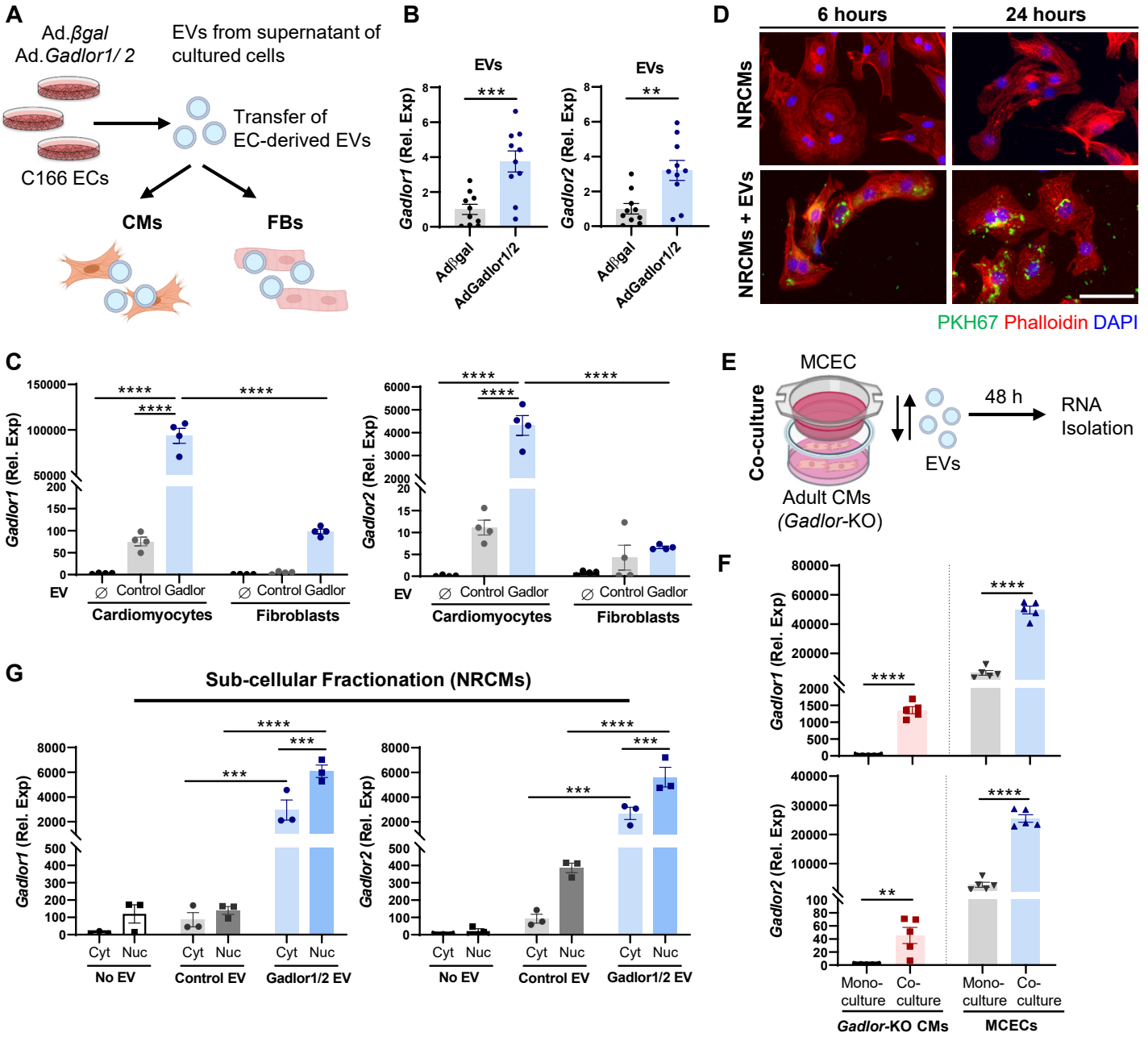

Figure 5: Secreted *Gadlor* lncRNAs are transferred to cardiomyocytes via endothelial-derived EVs.

A. Schematic representation of experimental design of EV (isolated from C166 endothelial cells, EC, supernatant) transfer to NRCMs or NRFBs. **B.** Validation of *Gadlor1* and *Gadlor2* overexpression in isolated EVs. **C.** RT-qPCR detection of *Gadlor1* and *Gadlor2* after transferring control EVs (isolated from Ad*βgal* treated ECs) or *Gadlor*-EVs (isolated from Ad*Gadlor1/* 2 treated ECs) on neonatal rat cardiomyocytes (NRCMs) or neonatal rat cardiac fibroblasts (NRFBs). The samples were collected after 6 hours of EV incubation. **D.** Visualization of NRCMs that were incubated with PKH67-labelled (green) EVs isolated from C166 ECs for 6 hours and 24 hours. Staining was performed with Phalloidin (red) and DAPI (blue). Scale bar: 50 µm. **E.** Scheme of co-culture experiment with transwell (1 µm pore diameter – allows EV transfer). Mouse cardiac EC (MCEC) on top cultured with *Gadlor*-KO CMs in the bottom well without direct cell contact. **F.** RT-qPCR detection of *Gadlor1* and *Gadlor2* in isolated *Gadlor*-KO CMs and MCEC mouse ECs after 48 hours of mono-culture or co-culture as indicated. **G.** *Gadlor1* and *Gadlor2* expression in the cytosol and nucleus of the recipient NRCMs after EV transfer (as shown in A). Data are shown as mean±SEM. Data normality was evaluated with Shapiro-Wilk test. P-values were calculated with Student's t-test or one-way ANOVA with Fisher's LSD post-hoc test for comparing two or multiple groups, respectively. Two-way ANOVA with Fisher's LSD post-hoc test was applied for grouped analysis when applicable. *p-value<0.05, **p-value<0.01, ***p-value<0.001, ****p-value<0.0001.

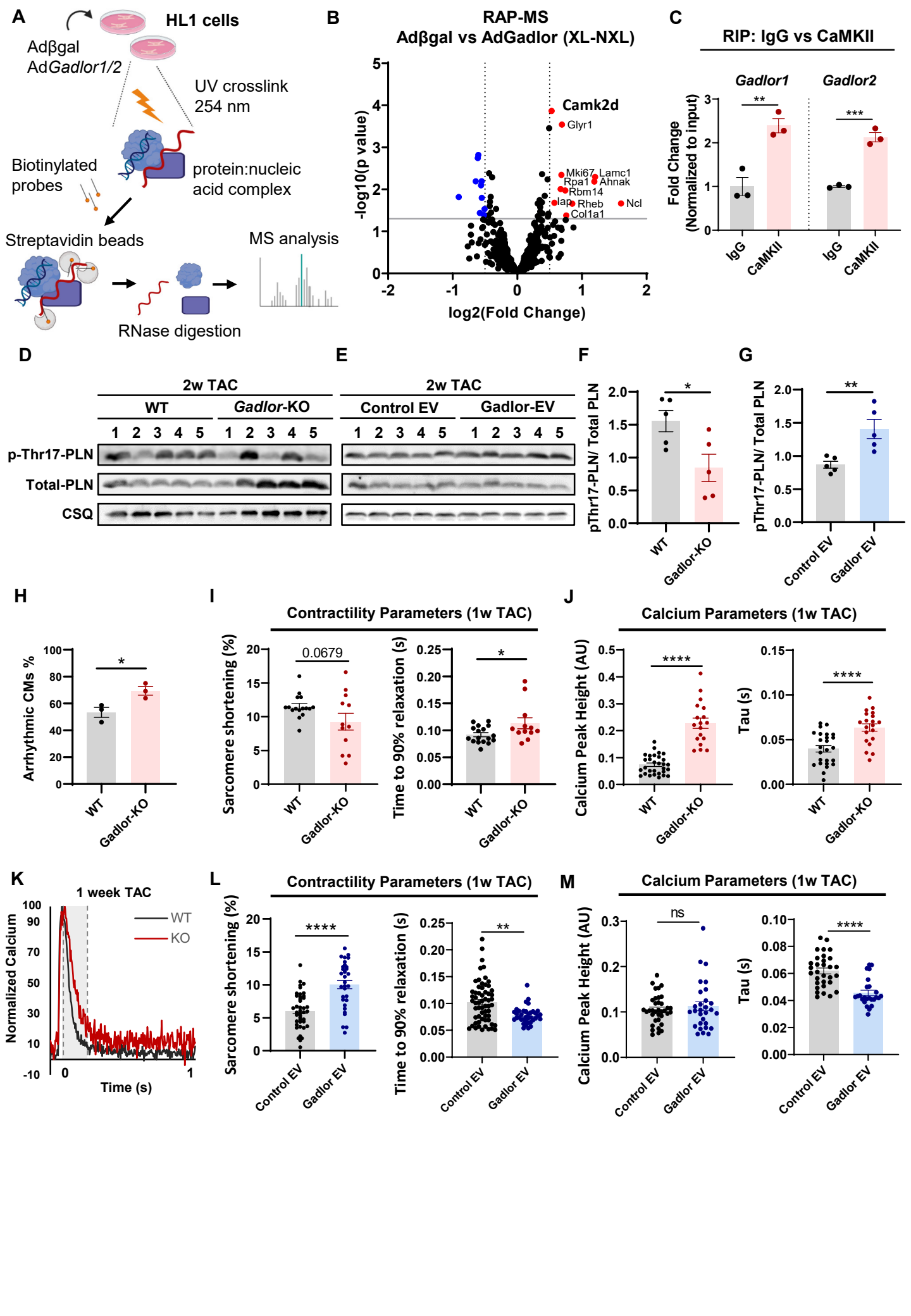
A
HL1 cells
Adβgal
AdGadlor1/2
UV crosslink
254 nm
Biotinylated
probes
protein:nucleic
acid complex
Streptavidin beads
MS analysis
RNase digestion
B
RAP-MS
Adβgal vs AdGadlor (XL-NXL)
Camk2d
Glyr1
Mki67
Lamc1
Rpa1
Ahnak
Rbm14
Iap
Rheb
Ncl
Col1a1
-log10(p value)
log2(Fold Change)
C
RIP: IgG vs CaMKII
Gadlor1
Gadlor2
Fold Change
(Normalized to input)
IgG
CaMKII
D
2w TAC
WT
Gadlor-KO
p-Thr17-PLN
Total-PLN
CSQ
E
2w TAC
Control EV
Gadlor-EV
F
pThr17-PLN/ Total PLN
WT
Gadlor-KO
G
pThr17-PLN/ Total PLN
Control EV
Gadlor EV
H
Arrhythmic CMs %
WT
Gadlor-KO
I
Contractility Parameters (1w TAC)
Sarcomere shortening (%)
0.0679
Time to 90% relaxation (s)
WT
Gadlor-KO
J
Calcium Parameters (1w TAC)
Calcium Peak Height (AU)
Tau (s)
WT
Gadlor-KO
K
1 week TAC
Normalized Calcium
WT
KO
Time (s)
L
Contractility Parameters (1w TAC)
Sarcomere shortening (%)
Time to 90% relaxation (s)
Control EV
Gadlor EV
M
Calcium Parameters (1w TAC)
ns
Calcium Peak Height (AU)
Tau (s)
Control EV
Gadlor EV

Figure 6. *Gadlor* lncRNAs bind to calcium/calmodulin-dependent protein kinase type II in cardiomyocytes.

A. Experimental scheme of RNA-antisense purification coupled with mass spectroscopy (RAP-MS) to identify specific interaction partners of *Gadlor1/2* in HL1 cardiomyocytes treated with βgal and *Gadlor1/2* adenovirus. **B.** Volcano plot indicating the identified interaction partners of *Gadlor1* and *Gadlor2* in cardiomyocytes with RAP-MS (Fold change enrichment (FC) threshold 1.2 and p-value < 0.05). UV crosslinking was used to stabilize protein:RNA interactions and non-crosslinked (N-XL) samples were used as background and removed from crosslinked (XL) samples for each indicated condition. **C.** RNA immunoprecipitation (RIP) performed with anti-IgG or anti-CaMKII antibodies from HL-1 cardiac muscle cell lysate to validate the interaction with *Gadlors*. RT-qPCR analysis showing the enrichment of *Gadlor1* and *Gadlor2* compared to IgG controls. Data was normalized to input RNA expression. (n=3 for each condition) **D-E.** Exemplary Western blots of phospho-Thr17-PLN and total PLN with CSQ as loading control in **(D)** WT and *Gadlor*-KO and **(E)** in control-EV and Gadlor-EV treated mouse heart tissue samples after 2 weeks TAC. **F-G.** Quantification of Western-blots. **H.** Percentage of isolated adult WT and *Gadlor-KO* cardiomyocytes with arrhythmic phenotype after 1-week TAC recorded by Multicell HT system (Ion-Optix) Cell number≥30 in each condition. Sarcomere contractility **(I-K)** and calcium transient **(L-M)** measurements were recorded in parallel with Multicell HT system with continuous perfusion of basal media on isolated adult CMs after 1-week TAC. **I.** Contractility parameters including sarcomere shortening (%) and relaxation. **J.** Calcium parameters including calcium peak height (arbitrary units, AU) and decay time (tau, seconds). **K.** Representative calcium transient recordings of WT and *Gadlor*-KO mice shown as normalized levels of calcium (%). **L.** Sarcomere function and **M.** calcium transient and decay time constant (tau). Recordings were obtained from adult cardiomyocytes isolated from WT mice after 1 week TAC followed by incubation of control-EV (Ad.βgal) and *Gadlor1/2*-EVs (Ad.Gadlor1 and Ad.Gadlor2) for 4-6 hours. Data are shown as mean±SEM. Data normality was evaluated with Shapiro-Wilk test and p-values were calculated with Student's t-test (Mann-Whitney for non-parametric) for comparing two groups. *p-value<0.05, **p-value<0.01, ***p-value<0.001, ****p-value<0.0001.

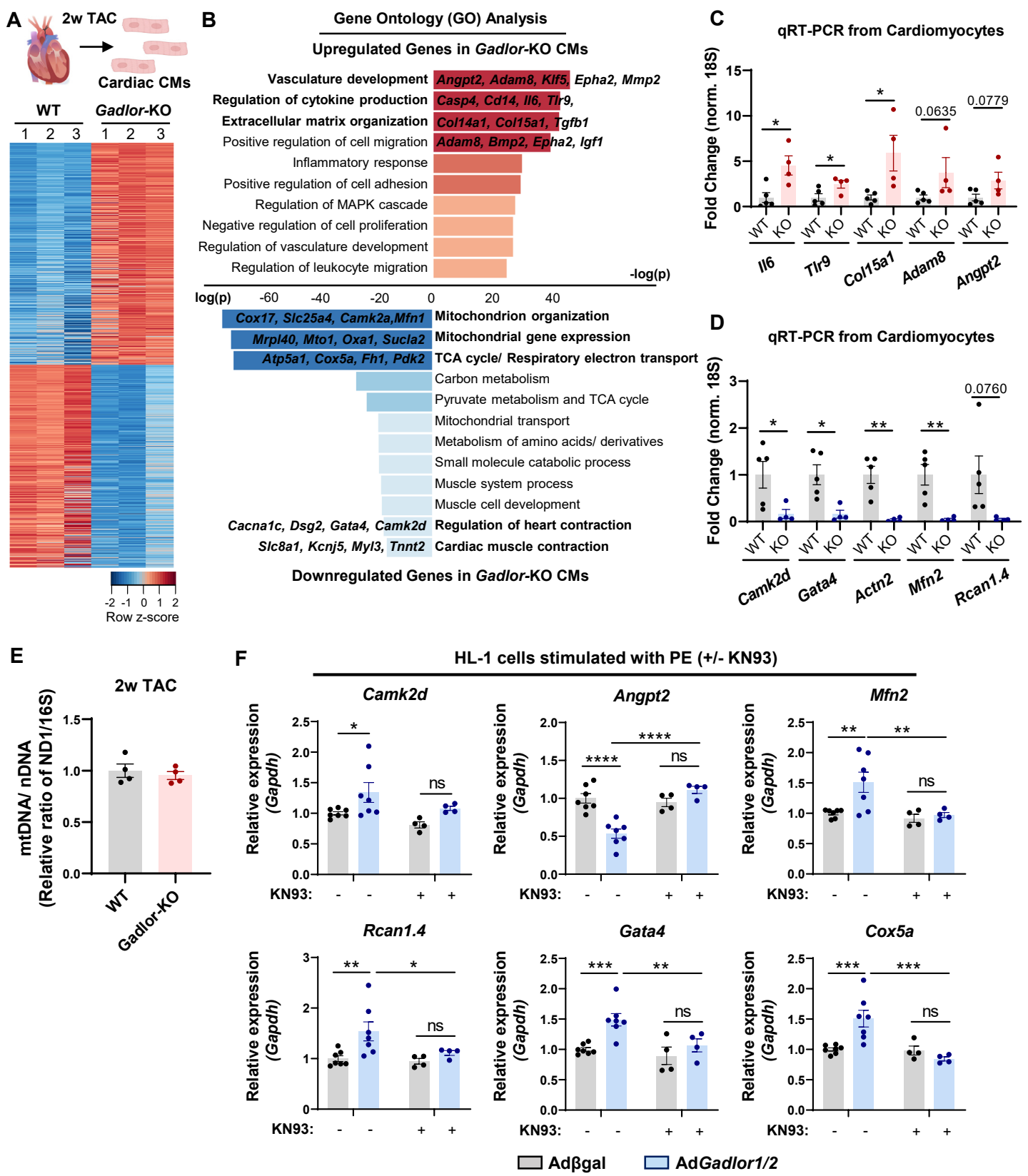

Figure 7. Deletion of *Gadlor1* and *Gadlor2* affects gene expression in cardiomyocytes.

A. Heatmap showing differentially regulated genes analysed by bulk RNAseq of isolated cardiomyocytes after 2-weeks TAC. **B.** Bar plots showing the gene-ontology (GO) analysis of upregulated and downregulated genes in *Gadlor*-KO CMs after 2-weeks TAC. (Red: Upregulated in *Gadlor*-KO, Blue: Downregulated in *Gadlor*-KO). Exemplary genes were listed for selected GO-terms. **C-D.** Validation of selected upregulated and downregulated genes from RNAseq data with qRT-PCR. **E.** Analysis of mitochondrial DNA (mtDNA) to nuclear DNA (nDNA) ratio determined via quantitative PCR by using WT and *Gadlor-KO* heart tissue samples isolated 2-weeks after TAC. Assessment of ND1 and 16S DNA abundance was used to determine the mtDNA/ nDNA ratio. **F.** qRT-PCR of selected genes in HL-1 cardiac muscle cells overexpressing *Gadlor* lncRNAs after *Gadlor1/2* adenovirus treatment (*βgal* as control) followed by phenylephrine (PE) stimulation (100 µM, 24 hours) with and without KN93 (1 µM, 2 hours) addition. Data are shown as mean±SEM. Data normality was evaluated with Shapiro-Wilk test. P-values were calculated with Student's t-test for parametric (or Mann-Whitney for non-parametric) for comparing two groups. Two-way ANOVA with Fisher's LSD post-hoc test was applied for grouped analysis. ns: no significance, *p-value<0.05, **p-value<0.01, ***p-value<0.001, ****p-value<0.0001.

Supplemental Material

Supplemental Methods

Human Tissue and Serum Samples

Studies on human heart tissue samples were approved by the Institutional Ethical Board of Massachusetts General Hospital (US). Human heart tissue samples were collected from patients with end-stage heart failure undergoing cardiac transplantation. Control heart tissue samples was obtained from healthy organ donors when the organ was not eligible for transplantation, or from the victims of traffic accidents. Human serum samples were obtained from healthy blood donors, or from aortic stenosis patients before replacement of the aortic valve, where all donors provided a written informed consent for the collection and use of samples, that had received approval from Institutional Review Board of Christian-Albrechts-Universität Kiel (File number: A174/09).

Measurement of GADLORs in Human Serum Samples

Human serum samples were collected on the day before Transcatheter Aortic Valve Implantation (TAVI). Serum-RNA was extracted using miRNeasy serum/plasma kit (#217184; Qiagen) based on manufacturer's instructions. LncRNA levels were normalized by the addition of 2 µl of TATAA universal RNA Spike (#RS10SII; Tataa Biocenter) prior to RNA-isolation. RNA was transcribed to cDNA (#K1652; Maxima H Minus First Strand cDNA Synthesis Kit; Thermo Fisher) and analyzed with TaqMan Non-coding RNA Technology (#4369016) using custom specific TaqMan Gene Expression Assay (#43331348, ID: APPRKET und APRWEYP; Thermo Fisher). For quantitative RT-PCR, the Stratagene's MX4000 multiplex qPCR system was used.

Animal Use and Experiments

All studies including the use and care of animals were performed with the permission of the Regional Council Karlsruhe and the Lower Saxony State Office for Consumer Protection and Food Safety, Germany, with approved protocols 35-9185.81/G-144/18, I-22/03, 33.9-42502-12-10/0016, 33.19-42502-04-14/1403 and 33.8-42502-04-16/2356.

Wildtype ICR/CD1 mice were in-bred in- house and C57BL/6N mice were obtained from Janvier Labs (Le Genest-Saint-Isle, France). Animals were maintained in a temperature-humidity controlled (22± 2°C and 35-60% humidity), 12-h dark-light cycled room with unlimited access to water and standard food.

Systemic *Gadlor* knock-out mice (*Gadlor*-KO) were generated by deletion of the respective region of mouse chromosome 16 using a CRISPR-Cas9 based strategy. Briefly, embryonic stem cells (G4 line, doi 10.1073/pnas.0609277104) were transfected with gRNAs LNC1-01 (target sequence: 5'-TTGTACATGAGCGGTTGTAG) and LNC2-01 (target sequence 5'-AGTATACAGGGGGTTACCAT) as well as in vitro transcribed CAS9-GFP mRNA. GFP expressing cells were sorted and single cell derived clones were established. 5 out of 72 analyzed clones showed extensive deletions between the gRNA target sites. Clone 1-37 comprised a deletion of 39995533 – 40004426 on one chromosome 16 allele. This clone was injected into C57BL/6 blastocysts to generate a transgenic mouse line which was then further crossed to achieve a homozygous deletion.

Transverse Aortic Constriction (TAC)

Transverse aortic constriction (TAC) was induced in 8-10 weeks old mice and maintained for 1-week or 2-weeks for short-term and 8-12 weeks for long-term studies. Analgesia (0.1 mg/kg buprenorphine) was provided by subcutaneous injection. Tracheal intubation was followed by upper thoracotomy to visualize the aortic arch, which was tied with a 7-0 silk ligature around a 26-gauge needle that was removed

immediately after secured constriction. Mice were injected with 0.1 mg/kg atropine, and the chest wall was closed with suture then followed with closure of skin with surgical glue. The mice were ventilated with 2% isoflurane throughout the procedure. For postoperative care, additional analgesia was provided in drinking water for the following 5 days. To assess the mortality rate, mice were followed and inspected daily after TAC. Sham operated animals were treated with the same procedure and medications, but no constriction was applied to aortic arch.

Transthoracic Echocardiography

Echocardiography was performed with 1% isoflurane anesthesia. Mice were dorsally placed on a heated table to maintain the body temperature during the procedure while the ECG and the respiration rate were recorded continuously. Echocardiography was recorded with a linear 30-40 MHz transducer (MX-550D) and the Vevo 3100 system (Visualsonics, Toronto, Canada). Data were analyzed with the VevoLab 5.5.0 software.

Left Ventricle and Apical four Chamber View. Parameters were recorded in B-mode and M-mode in both parasternal long axis (PSLAX) and short-axis (SAX) view at the papillary muscle level. Left-ventricular posterior wall thickness and left-ventricular end-diastolic volume were used to characterize LV microanatomy (LVPW and LVEDV) and the change of LV diameter length from end-diastole (LVID) to end-systole was used to assess contractility and to calculate LV ejection fraction and fractional shortening (LV-EF and LV-FS), which were measured with the PSLAX mode in the analysis. B-mode tracing in the apical four-chamber view was recorded at the atrioventricular valve level with pulse wave-Doppler (PW-Doppler) and tissue-Doppler measurements.

Carotid flow measurement. To evaluate the degree of aortic constriction during TAC surgery, the peak velocity of flow in the right and left common carotid arteries (RCCA and LCCA) were measured 2 days after surgery with PW-Doppler at the level of carotid bifurcation to calculate the ratio of RCCA/LCCA flow.

Organ Harvest

At the end of the experiment, mice were weighed and euthanized to collect the heart, lungs and liver. Organs were washed in cold PBS to remove the blood, and additionally the heart was washed in 0.5% (w/v) KCl in PBS. The heart was transversely cut into half, and the upper layer was immediately embedded into OCT for histological analysis while the other half was snap-frozen.

Histology

OCT embedded organs were sectioned into slices of 7 µm and 12 µm for immunofluorescence and Picro-Sirius red staining, respectively. Briefly, for immunofluorescence tissue sections were fixed with 4% PFA followed by permeabilization with 0.3% Triton-X in PBS, and blocking with 3% BSA. Primary and secondary antibodies that were used are listed in **Supplemental Table 2**. Samples were visualized with Leica DMi8 Fluorescence microscope. Images were analyzed with Leica Application Suite X (LAS X) 3.7.

Sirius red staining was performed by fixing the tissue samples with 100% ice-cold acetone, and by following the standard protocol. Tissue sections were scanned with Zeiss Axio Scan.Z1. Images were analyzed with ZEN 2.6 Blue Edition, Carl Zeiss.

Isolation and Culture of Juvenile Mouse Endothelial Cells (mECs)

Hearts from 7-12 days old mice were collected and washed in ice-cold DMEM high-glucose to clean and remove the atria. The minced tissue was transferred into 5 ml of enzyme solution (for 3-4 hearts) and incubated with collagenase I (500 U/ml, Worthington - LS004176) and DNase I (150 U/ml, Worthington - LS002139) in HBSS (without Ca and Mg). After digestion, the lysate was washed with FCS and passed through a 70 µm cell strainer. Washed lysate was incubated with CD31 antibody (BD, 553370) coupled to Dynabeads (Invitrogen, 11035) for the first step of isolation, before the cells were plated on 0.5% gelatinized plates. For culturing, cells were maintained for 3-4 days until they reached 80-90% confluency. During the first passage, further purification of cells was achieved by incubation with CD102 antibody (BD, 553370) coupled Dynabeads. Primary endothelial cells were maintained in DMEM with 20% FCS supplemented with non-essential amino-acids and sodium pyruvate, and passaged up to P3 for experiments.

Isolation of Adult Mouse Endothelial Cells, Fibroblasts and Cardiomyocytes

Isolation of endothelial cells and fibroblasts from adult mouse heart was performed with MACS-magnetic beads from Miltenyi Biotec. Briefly, heart tissue was washed in ice-cold PBS, minced into small pieces before incubating in enzyme solution (collagenase I (500 U/ml, Worthington - LS004176) and DNase I (150 U/ml, Worthington - LS002139) in RPMI 1640 (Thermo Fischer Scientific: 31870025)). Digested tissue samples were passed through a 0.70 µm cell strainer and washed with FCS, and MACS buffer with BSA (Miltenyi Biotec, 130-091-222). After multiple washing steps, the tissue lysate was incubated with CD146 microbeads (Miltenyi Biotec, 130-092-007) before being passed through magnetic columns (Miltenyi Biotec, MS columns 130-042-201) for positive selection of endothelial cells (EC). The flow through was incubated with feeder removal microbeads (Miltenyi Biotech, 130-095-531) and eluted after multiple washing steps to collect fibroblasts (FB). Isolated cells were stored as frozen cell pellet for later RNA or

protein isolation for corresponding experiments.

Isolation of adult cardiac myocytes was achieved by using a Langendorff perfusion system.[1] Briefly, immediately after excision, the heart was placed into ice-cold 1x perfusion buffer (10x stock: 1130 mM NaCl ,47 mM KCl, 6mM KH_2PO_4, 6 mM Na_2HPO_4, 12 mM $MgSO_4.7H_2O$, 120 mM $NaHCO_3$, 100 mM $KHCO_3$, 100 mM HEPES buffer solution and 300 mM Taurine) to clean the tissue around the aorta under a microscope. Then the aorta was placed onto a cannula (inner diameter 1mm) with forceps and tied with silk suture to allow perfusion through the coronary arteries. Subsequently, the heart was perfused with enzyme solution containing Liberase DH (5 mg/ml, Roche, 5401089001), trypsin (1%, Gibco, 15090046) and $CaCl_2$ (100 mM) to digest the tissue at 37°C. Enzymatic digestion was ended with Stop I and II solutions containing perfusion buffer with FCS and $CaCl_2$ (10 mM). Digested heart tissue samples were passed through a 100 µm cell strainer. Then, the calcium concentration was gradually increased by manual administration to digested heart tissue with continuous gently mixing. Then the cells were subjected to either IonOptix analysis, culturing or direct RNA and protein extraction (after cardiomyocyte sedimentation).

Isolation of Neonatal Rat Cardiomyocytes (NRCMs)

Hearts from 1-3 days old rats were collected and washed with ice-cold 1x ADS (pH 7.35) to clean the blood and remove the atria. The ventricular parts were minced in 1x ADS and digested in enzyme solution containing collagenase Type II (Worthington: LS004176) and pancreatin (Sigma P3292). The resulting cells were loaded onto a Percoll gradient to separate cardiomyocytes (NRCMs) and non-cardiomyocytes. NRCMs were seeded (4.0×10^5 /well for 6 well-plate) onto 0.5% gelatin coated plates.

Isolation of Extracellular Vesicles (EVs)

Isolation of EVs were performed with ultracentrifugation from the supernatant of C166 cells that were cultured with EV depleted FCS. Initially, cell debris and large vesicles (apoptotic bodies) were removed by centrifugations at 300xg and 10.000xg, respectively. Subsequently, small EVs (including microvesicles and exosomes) were collected with 100.000xg ultracentrifugation for 90 minutes, and similarly washed with PBS, before a second round of centrifugation was performed. The EV pellet was re-suspended in PBS for NTA (ZetaView Nanoparticle Tracing Videomicroscope, PMX-120) measurements, or with QIAzol lysis buffer (Qiagen, 79306) for RNA isolation.

EV-RNA isolation. RNA isolation from EVs was performed by RNA precipitation as described before.[2] Briefly, the EV pellet was resuspended with 1 ml of QIAzol, and then mixed with 200 µl of chloroform for phase separation. Samples were mixed thoroughly and incubated for 5 minutes in room temperature (RT), then centrifuged at 12.000xg at 4°C for 15 minutes. The aqueous upper layer was mixed with 10% (v/v) sodium acetate (3M, pH 5.5) and 4 µl of glycogen (5 mg/ml) in 1.5 ml ethanol (100%). Samples were incubated at -80°C overnight, then centrifuged at 16.000xg for 30 minutes to pellet the RNA. The RNA pellet was then washed with 70% ethanol and dried, before being re-suspended in nuclease-free water.

EV RNase and Proteinase-K Protection Assay. To test the transfer of *Gadlor* lncRNAs within EVs, we performed RNase and proteinase K protection assays with and without prior the application of Triton-X. In brief, EVs were isolated and treated with 100 ng/µl of RNase A, and 20 mg/µl of proteinase K for 30 minutes at 37°C. 5mM of PMSF was used to inactivate the proteinase K at RT. To disrupt the lipid bilayer, EVs were incubated with 1% Triton-X for 1 hour for selected samples. As a negative control, RNA isolated from EVs was also treated with the same protocol.

EV-labelling with PKH67 cell linker. To visualize EVs for transfer and re-uptake experiments *in vitro,* they were labelled with PHK67 Green Fluorescent Cell Linker kit (Sigma MIDI67). Briefly, EV pellet was re-suspended with 1 ml of diluent C including 4 µl of PKH67 dye, and incubated for 5 minutes at RT. Then 1%

BSA-PBS was added into the suspension to remove the unspecific binding of the dye. Then EVs were pelleted at 3000xg for 1 hour, which were then suspended with the cell culture medium and added on NRCMs. Visualization of EVs was conducted with the Leica Confocal Microscope TCS SP8 and images were analyzed by Leica Application Suite X (LAS X) 3.7.

EV FACS Staining. Characterization of surface markers of EVs was performed with flow cytometry by staining EC-derived EVs with CD9-PerCP-Cy5.5 (Miltenyi Biotec, 130-102-278, Clone: MZ3), CD63-APC (Miltenyi Biotec, 130-108-894, Clone: REA563) and CD54-FITC (BD, 553252, Clone: 3E2) labelled antibodies for 1 hour at 4°C. Measurements were obtained with BD FACSCanto ll.

EV Transmission Electron Microscopy (TEM). Visualization of EVs were performed with TEM. After centrifugation, pellets were resuspended in the minimum possible volume of residual liquid and 25 % aqueous glutaraldehyde was added to a final concentration of 1 %. After fixation overnight, samples were mixed 1:1 (v/v) with 4 % agar at 40 °C. After hardening, the agar blocks were cut to cubes of 1 mm size. Further preparation of samples and electron microscopy were performed as described, before being imaged with a FEI Morgagni 268 transmission electron microscope (FEI, Eindhoven, Netherlands) operated at 80 kV using a Veleta CCD camera (Olympus Soft Imaging Solutions).[3]

EV-mediated Gadlor1 and Gadlor2 overexpression. As a gain-of-function approach, *Gadlor1* and *Gadlor2* were overexpressed in mouse hearts by administration of *Gadlor1/2*-enriched EVs. To this end, C166 endothelial cells were infected with *Gadlor1* and *Gadlor2* adenoviruses for 48 hours. EVs were collected with ExoQuick-TC solution (EXOTC50A-1,65 SystemsBio) based on manufacturers' protocols with some adjustments. In vivo overexpression of *Gadlor* lncRNAs was achieved by injecting EVs directly into the left ventricles before TAC surgery. Intra-ventricular injection was performed by simultaneous cross-clamping of the aorta and pulmonary artery distal of the origin of the coronary vessels.

Cell Culture

C166 (CRL-2581, ATCC) mouse embryonic endothelial cells and NIH3T3 (CRL-1658, ATCC) mouse fibroblast cells were cultured in Dulbecco's Modified Eagle's Medium (DMEM) with 10% FCS, while MCECs (CLU510-P, Tebu-bio), immortalized mouse cardiac endothelial cells, were cultured with 5% FCS containing DMEM supplemented with L-glutamine (1%), penicillin/ streptomycin (1%) and HEPES. HL-1 cardiac muscle cells (SCC065, Merck) were cultured with Claycomb media (Sigma, 51800C) supplemented with 10% FCS, 0.1 mM norepinephrine, 2 mM L-glutamine and 1X penicillin-streptomycin (P/S). HL-1 cells were plated on 0.1% gelatin coated flasks, and cell culture media was refreshed daily. Cells were cultured for up to 10 passages.

Adenoviral infection. For overexpression of *Gadlor* lncRNAs, recombinant adenoviruses were used. Mouse cDNAs of AK037972 (*Gadlor*1) and AK038629 (*Gadlor*2) were subcloned into the pShuttleCMV vector (Source Bioscience, UK) and adenoviruses were generated by the AdEasy Adenoviral Vector system (Agilent, 240009). An adenovirus overexpressing β-Galactosidase (Ad*ßgal*) was used as control. After production of adenoviruses, the viral titer was calculated with the help of the AdEasy Viral Titer Kit (Agilent, 972500), and all the experiments were performed with 50 MOI. Adenoviral infection on cultured cells was performed for 4 hours at 37°C on cells with media containing heat-inactivated FCS.

Co-culture experiments. For co-culture experiments, adult mouse cardiomyocytes isolated from *Gadlor*-KO mice were seeded on laminin (Santa Cruz, SC-29012) coated 6-well plates and cultured with MCECs plated on 1 µm pore-sized inserts (Thincert, Greiner, 657610). Cells were collected separately after 48 hours for RNA isolation.

Endothelial-cell Sprouting Assay

To study the effect of *Gadlor* lncRNAs on angiogenesis, we performed sprouting assays with C166 mouse ECs according to a well-established protocol previously described.[4] Briefly, cells were infected with *Ad. ßgal or Ad.Gadlor1/2* adenovirus for 24 hours. 50.000 cells were re-suspended with 4 mL DMEM + 10 % FCS and 1 mL methylcellulose solution (Sigma-Aldrich, M0512) and drops containing 25 µl of suspension were pipetted onto a 10 cm cell culture dish. The drops were then incubated upside-down in a cell culture incubator for 24 hours to allow spheroid formation. On the following day, the cell spheroids were gently washed off the hanging drops with PBS, collected by 200xg centrifugation for 5 minutes and re-suspended with methylcellulose solution containing 20 % FCS. Collagen matrix was prepared in parallel on ice with collagen stock solution (Corning, 11563550), diluted in 10x M199 medium (Sigma-Aldrich, M0650) and the required amount of sodium hydroxide to set the pH for polymerization. Then the collagen medium was mixed to the spheroids. 1 mL of the spheroid-collagen-methylcellulose mixtures were added per well in a 24-well plate and incubated in a cell culture incubator for 30 min to induce the polymerization of the collagen-methylcellulose matrix. The endothelial spheroids were stimulated with 100 µl of DMEM + 10 % FCS, 25 ng/mL FGF2 or 10 ng/mL TGF-β1 by adding it dropwise to the collagen matrix. After 24 hours, the sprouting assay was stopped by adding 1 mL of 4% paraformaldehyde to the wells. Spheroids were visualized with the 10X objective in bright-field microscopy and analyzed with ImageJ.

RNA Isolation and qRT-PCR

RNA isolation from tissue samples was performed with QIAzol reagent (Qiagen, 79306), and from isolated cells with NucleoSpin RNA isolation kit (Macherey-Nagel, 740955.250) according to manufacturers' protocols. cDNA was generated by using the Maxima H minus First stand cDNA synthesis kit (Thermo Fisher Scientific, K1652). Quantitative PCR was performed with the Maxima SYBR Green mix with ROX as reference dye (Thermo Scientific, K0253) on an AriaMx Real-time PCR System (Agilent, G8830a). Gene

expression was normalized to *Gapdh*,18S or *U6* expression. All qPCR primer sequences are listed in the **Supplemental Table 3**.

Protein Isolation and Western blotting

Heart tissue protein lysates were prepared from frozen pulverized tissue with lysis buffer containing 30 mM Tris-pH 8.8, 5 mM EDTA-pH 8.0, 3% SDS (v/v), 10% glycerol (m/v), protease and phosphatase inhibitors. Protein quantification was performed by BCA assay (ThermoFisher, Pierce BCA Protein Assay kit, 23225). Samples were incubated at 95°C for 5 minutes after addition of Laemmli buffer (1X final concentration) and proteins were separated with SDS-PAGE electrophoresis. The following primary antibodies were used: Calsequestrin (Thermo Scientific PA1-913, rabbit), Phospholamban, pThr17 (Badrilla A010-13, rabbit), Phospholamban (Badrilla, A010-14 mouse). The following secondary antibodies were used: Rabbit anti-mouse peroxidase (Sigma-Aldrich), goat anti-rabbit peroxidase (Sigma-Aldrich).

Sarcomere Contractility and Calcium Transient Measurements

Adult cardiomyocytes were isolated 1-week after TAC operation. Cardiomyocytes were plated on laminin coated (10 µg/cm^2) 35 mm dishes (MatTek 10 mm Glass bottom dishes, P35G-1.5-10-C) and gently washed 1 hour later with MEM medium without butanedione monoxime (BDM). The plated cells were then transferred into the Ion-Optix Multicell High-throughput System chamber, where they were simultaneously paced (18 V, 2.5 Hz, 4 ms impulse duration), and assessed for sarcomere length and contraction. Calcium handling was recorded after incubation with 1 µM fura-2, AM (Invitrogen, F1221).

For measurements following *Gadlor1/2* overexpression via EV-mediated transfer, isolated adult cardiomyocytes were incubated with EVs for 4 hours. To assess the effect of CaMKII inhibition, cells were

treated with KN93 (1 µM) for 1 hour before the measurements. The recordings were analyzed with IonWizard software.

RNA antisense purification coupled with mass spectrometry (RAP-MS)

To identify the protein interaction partners of *Gadlor* lncRNAs we performed RAP-MS as described previously with minor modifications.[5] The 5' biotinylated antisense *Gadlor1* and *Gadlor2* probes were pooled in the experiment and the sequences are listed in **Supplemental Table 4**. We used HL-1 cardiomyocytes overexpressing *Gadlor1* and *Gadlor2* after infection with Ad.Gadlor1 and Ad.Gadlor2. RNA antisense purification (RAP) was performed with cells collected from five 15 cm dishes per sample, where each experimental group contained three replicates without (as a negative control to identify non-specific 'background' proteins) and four replicates with UV cross-linked conditions. HL-1 cells were washed with cold PBS twice and cross-linked using 150 mJ/cm^2 of 254 nm UV light. Cells were then lysed with lysis buffer, incubated 10 minutes on ice, homogenized by passing several times through a 21G needle and DNA was digested with addition of DNase salt solution and Turbo DNase for 10 minutes at 37°C (ThermoFisher, AM2238). Hybridization conditions were adjusted by the addition of an equal amount of hybridization buffer. Lysates were precleared with streptavidin-coated magnetic beads. Biotin labelled Gadlor1 and Gadlor2 probes were heated to 85°C for three minutes and then incubated with the lysate for 2 hours at 67°C. Probe-RNA complexes were captured by pre-washed streptavidin coated magnetic beads and incubating at 37°C for 30 minutes. Lysate was removed from beads by magnetic separation, and beads were washed four times in hybridization buffer at 67°C. *Gadlor* RNA bound proteins were then released by Benzonase RNA digestion for two hours at 37°C. The captured protein samples were identified by TMT labelling followed by liquid chromatography-mass spectroscopy (LC-MS/MS) by the EMBL proteomics core facility.

RNA immunoprecipitation (RIP)

We performed RIP with minor modifications to a previously described protocol to confirm the interaction of *Gadlor1* and *Gadlor2* lncRNAs with CaMKII. [6] HL-1 cardiomyocytes were used to overexpress *Gadlor* lncRNAs by adenovirus treatment, while Ad.βgal treated samples were used as control. Three 15 cm plates were combined for preparation of each sample. Briefly, cells were washed with ice-cold PBS twice and lysed with polysome lysis buffer (100 mM KCl, 5 mM MgCl2, 10 mM HEPES pH 7, 0.5% IGEPAL CA-630, 0.1 mM DTT, 1 x protease inhibitor cocktail, 1 x RNasIN). Cell lysates were passed through a 26G needle multiple times for homogenization. Protein G magnetic beads (Bio-Rad SureBeads, 161-4221) were washed twice with NT-2 buffer (50 mM Tris-HCl pH 7.4, 150 mM NaCl, 5 mM MgCl2, 0.05 % IGEPAL CA-630) and coupled with anti-CaMKII antibody (Santa Cruz, sc-5306) or anti-IgG (mouse, Cell Signaling 7076, as control) overnight at 4°C. Antibody coupled beads were washed twice with NT-2 buffer and resuspended in NET-2 buffer (50 mM Tris-HCl pH 7.4, 150 mM NaCl, 5 mM MgCl2, 0.05 % IGEPAL CA-630, 20 mM EDTA pH 8, 1 mM DTT, 1 x RNaseIN). Cell lysates were added to beads and incubated at 4°C for 2 hours (10% lysate was removed as input and stored on ice prior to IP).

After supernatant was removed from beads, 1 ml of ice-cold NT-2 buffer was used to wash the beads five times in total. Then, beads were resuspended with Proteinase K buffer (1x NT-2 buffer and 1% SDS) and incubated at 55°C for 30 minutes with constant shaking while input sample conditions were adjusted accordingly and processed in parallel. Supernatant was transferred into fresh tubes and combined with NT-2 buffer and UltraPure phenol-chloroform (ThermoFisher, 15593031) for RNA purification. After centrifugation in heavy-lock tubes at 15.000 x g for 15 minutes, RNA was purified from the clear aqueous phase with the RNA Clean and concentrator kit (Zymo Research, R1017).

RNAScope *in situ* Hybridization

In situ hybridization was performed to localize Gadlor1 (Mm-LOC118567341-C3), Gadlor2 (Mm-AK038629-C1, Cat no: 404391) and Cdh5 (Mm-Cdh5-C2, Cat no: 312531) mRNA expression on mouse heart tissue slides with RNAscope Multiplex Fluorescent v2 kit. The assay was performed according to the manufacturers' protocol. Briefly, OCT-embedded tissue slides (7 µm thickness) were used in the assay, fixed with 4% PFA and then stepwise dehydration was performed with increasing concentrations of ethanol. Tissue slides were subsequently treated with hydrogen peroxide (10 min at RT) and protease IV (30 min at RT) in the humidity control incubator. Slides were incubated for 2 hours with the mixture of probes to hybridize with the corresponding RNAs. Next, the signal was amplified with RNAScope Multiplex FL v2 AMP 1-3 reagents and then HRP channels were developed sequentially. Finally, DAPI was used to counterstain the slides and each was mounted with ProLong Gold Antifade Mountant (Fisher Scientific).

DNA Isolation and Analysis of mtDNA/ nDNA

To analyze the mitochondrial DNA (mtDNA) to nuclear DNA (nDNA) ratio of *Gadlor*-KO and WT mouse hearts after 2-weeks of TAC, genomic DNA was isolated from mouse heart tissue samples obtained after TAC (2w) with a DNA isolation kit according to manufacturers' instructions (PureLink Genomic DNA Mini kit, Invitrogen, K182001). The mtDNA/ nDNA ratios were quantified by quantitative PCR using ND1 and 16S rRNA primers listed in the **Supplemental Table 3**.

Bulk RNA sequencing and Bioinformatics

In order to perform RNA sequencing, RNA isolation was performed from isolated cells as described at indicated time-points (2 weeks after TAC or sham surgery). Quality control of RNA samples (Agilent 2100 Fragment Analyser), and library preparation (DNBSEQ Eukaryotic Strand-specific mRNA library) were

performed by BGI, Hong Kong. Bulk RNA sequencing from different cardiac cells were performed as stranded and single-end with 50 base sequence read length by BGI with Illumina HiSeq 2500. Initially, the trimming of adapter sequences from Fastq files was performed with the R package *FastqCleaner*. For aligning the reads to the reference genome (mm10) after trimming, the R package *bowtie2* alignment tool was used. Gene annotation was performed with *bioMaRt* R package. Library size of the samples were normalized to counts per million (cpm), and transformed into log2 values followed by calculation of differential gene expression with the *edgeR* package of R. Significant changes in gene expression between compared groups were filtered based on FDR < 0.05, and fold change (FC) > 1.5. Gene ontology analysis were performed with Metascape and DAVID online tools. Heatmaps that show the differentially regulated genes were generated by heatmap.2 function in *ggplot2* library in R.

RNAseq data-set is deposited in National Center for Biotechnology Information's Gene Expression Omnibus database with accession number GSE213612.

Statistics

Data analysis and statistical analysis were performed with GraphPad Prism software (Version 8). Data are shown as mean ± standard error of the mean (SEM). All the experiments were carried out in at least 3 biological replicates. The number of replicates for animal experiments and cell culture experiments are indicated in the figure legends. The investigators were blinded for mouse genotype and treatment during surgeries, echocardiography, organ weight determination and all histological and immunofluorescence quantifications.

Initially, all the datasets were analyzed for normality to allow the application of the proper statistical test. An unpaired 2-tailed Student t-test was used for comparing 2 groups only. Comparing multiple groups for one condition was performed with one-way ANOVA and Fisher's LSD post-hoc test. Comparing multiple

groups for multiple conditions was achieved with two-way ANOVA and followed with Fisher's LSD post-hoc test when applicable. For non-parametric data sets, the Mann-Whitney and Kruksal-Willis tests were used to compare two groups and multiple groups, respectively. Values of $p<0.05$ were considered statistically significant.

Method References

1. Louch WE, Sheehan KA, Wolska BM. Methods in cardiomyocyte isolation, culture, and gene transfer. *J Mol Cell Cardiol*. 2011;51:288-298. doi: 10.1016/j.yjmcc.2011.06.012
2. Prendergast EN, de Souza Fonseca MA, Dezem FS, Lester J, Karlan BY, Noushmehr H, Lin X, Lawrenson K. Optimizing exosomal RNA isolation for RNA-Seq analyses of archival sera specimens. *PLoS One*. 2018;13:e0196913. doi: 10.1371/journal.pone.0196913
3. Grund A, Szaroszyk M, Korf-Klingebiel M, Malek Mohammadi M, Trogisch FA, Schrameck U, Gigina A, Tiedje C, Gaestel M, Kraft T, et al. TIP30 counteracts cardiac hypertrophy and failure by inhibiting translational elongation. *EMBO Mol Med*. 2019;11:e10018. doi: 10.15252/emmm.201810018
4. Tetzlaff F, Fischer A. Human Endothelial Cell Spheroid-based Sprouting Angiogenesis Assay in Collagen. *Bio Protoc*. 2018;8:e2995. doi: 10.21769/BioProtoc.2995
5. McHugh CA, Guttman M. RAP-MS: A Method to Identify Proteins that Interact Directly with a Specific RNA Molecule in Cells. *Methods Mol Biol*. 2018;1649:473-488. doi: 10.1007/978-1-4939-7213-5_31
6. Gagliardi M, Matarazzo MR. RIP: RNA Immunoprecipitation. *Methods Mol Biol*. 2016;1480:73-86. doi: 10.1007/978-1-4939-6380-5_7

1 **Supplemental Tables**

2 **Table 1:** List of primers used for genotyping of *Gadlor*-KO mouse line

	Primer 1 (Forward)	**Primer 2 (Reverse)**
***Gadlor*-WT**	CTTGAGCCGTCTCTCCAAAG	GGGTGGCATGCAAGATGATTGAGA
***Gadlor*-KO**	CTTGAGCCGTCTCTCCAAAG	TGTGGAGTGGACACATAGAGG

3

4 **Table 2:** List of antibodies/reagents used in cell isolation methodologies and immunofluorescence (IF)

5 staining.

Target	**Company, Catalogue No**	**Application**
Anti-mouse CD146 (LSEC) MicroBeads	Miltenyi-Biotec, 130-092-007	Cell isolation
Feeder Removal MicroBeads, Mouse	Miltenyi-Biotec, 130-095-531	Cell isolation
Isolectin B4 (IB4)	Vector Lab, FL-1201	1:50 (IF)
Purified Rat Anti-mouse CD102	BD Pharmingen, 553326	Cell isolation
Purified Rat Anti-mouse CD31	BD Pharmingen, 553370	Cell isolation
Rabbit Polyclonal anti-ki67	Abcam, ab15580	1:100 (IF)
VECTASHIELD HardSet Antifade Mounting Medium With DAPI	Vector Lab, H-1500	
Wheat Germ Agglutinin (WGA)	Invitrogen, W21405	1:100 (IF)

6

7 **Table 3:** List of primers used for qPCR and qRT-PCR (5´-3´).

	Primer 1 (Forward)	**Primer 2 (Reverse)**
Gadlor1	AGGTGAGCTCTGGTTGTGTT	CTGCTGCCTGTGAAAGATGG

Gadlor2	TGAGACTCCACTTGCCACAT	TGTGGTTTCAGGCATGTTTCT
GADLOR1	AATTTCAGCCACAAGCATCC	TGCTTGGGGAAGAGGAAGTA
GADLOR2	TGGGATCTAAGCACTGACACC	GAGACAGACATTCGTTTGGTCA
18S	GTAACCCGTTGAACCCCATT	CCATCCAATCGGTAGTAGCG
U6	CTCGCTTCGGCAGCACA	AACGCTTCACGAATTTGCGT
Gapdh	CGTCCCGTAGACAAAATGGT	GAATTTGCCGTGAGTGGAGT
Acat1	GCAGGGAAGTTTGCCAGTGAGA	GAACACGGTCTTGAGCTTTGGC
Actn2	CACCTGGAGTTTGCCAAGAGAG	GCCTTGAACTGCTCATGTGCAG
Adam8	TGCCAACGTGACACTGGAGAAC	GCAGACACCTTAGCCAGTCCAA
Angpt2	AACTCGCTCCTTCAGAAGCAGC	TTCCGCACAGTCTCTGAAGGTG
Angptl4	CTGGACAGTGATTCAGAGACGC	GATGCTGTGCATCTTTTCCAGGC
Aurkb	CTTCTACGACCAGCAGAGGATC	GGCATCTGACAGTTCCTCCATG
Cacna1c	CGTTCTCATCCTGCTCAACACC	GAGCTTCAGGATCATCTCCACTG
Camk2d	GTGACACCTGAAGCCAAAGACC	CCTGTGCATCATGGAGGCAACA
Cdk1	CATGGACCTCAAGAAGTACCTGG	CAAGTCTCTGTGAAGAACTCGCC
Col15a1	ACACCCACAGTGACTCCCAAGA	TCCTCATTGCCCACGATGTCTC
Col1a1	CCGCTGGTCAAGATGGTC	CCTCGCTCTCCAGCCTTT
Col3a1	ATAAGCCCTGATGGTTCTCG	ATGCATGTTTCCCCAGTTTC
Col4a1	ATGGCTTGCCTGGAGAGATAGG	TGGTTGCCCTTTGAGTCCTGGA
Col6a1	GACACCTCTCAGTGTGCTCTGT	GCGATAAGCCTTGGCAGGAAATG
Comp	GTGCCCAACTTTGACCAGAGTG	ACAGGCATCACCCACAAAGTCG
Cox5a	GTCACACGAGACAGATGAGGAG	CCGTCTACATGCTCGCAATGCA
Cxcl2	CATCCAGAGCTTGAGTGTGACG	GGCTTCAGGGTCAAGGCAAACT
Dll1	GCTGGAAGTAGATGAGTGTGCTC	CACAGACCTTGCCATAGAAGCC

Efna1	GCTGAAGGTGACTGTCAATGGC	CGGCACTGTAACCAATGCTGTG
Fgfr2	GTCTCCGAGTATGAGTTGCCAG	CCACTGCTTCAGCCATGACTAC
Fh1	GAACTCACACGCAGGATGCTGT	GGCGGCTTTTATTCTCACCATCG
Fn1	TGTGACAACTGCCGTAGACC	TGGGGTGTGGATTGACCTTG
Gata4	GCCTCTATCACAAGATGAACGGC	TACAGGCTCACCCTCGGCATTA
Icam5	ACCGATGCACAGCAGTCAATGG	ATGTTCTGGGCAGCCTACACTG
Igf1	GTGGATGCTCTTCAGTTCGTGTG	TCCAGTCTCCTCAGATCACAGC
Il6	CGGCCTTCCCTACTTCACAA	TCCAGTTTGGTAGCATCCATCA
Klf15	ACACCAAGAGCAGCCACCTCAA	GCCTTGACAACTCATCTGAGCG
Lsamp	GGAGTCGAAGAGCAACGAAG	AATCTCAAGGCCATTTGCAC
Mfn2	GTGGAATACGCCAGTGAGAAGC	CAACTTGCTGGCACAGATGAGC
Myh6	GAGTGGGAGTTTATCGACTTCG	CCTTGACATTGCGAGGCTTC
Myh7	ACTGTCAACACTAAGAGGGTCA	TTGGATGATTTGATCTTCCAGGG
Nppa	TTCCTCGTCTTGGCCTTTTG	CCTCATCTTCTACCGGCATC
Nppb	GTCCAGCAGAGACCTCAAAA	AGGCAGAGTCAGAAACTGGA
Rcan1.4	CTTGTGTGGCAAACGATGATG	TGGTGTCCTTGTCATATGTTCTG
Sirt1	GGAGCAGATTAGTAAGCGGCTTG	GTTACTGCCACAGGAACTAGAGG
Sucla2	GGTGTCTCTGTTCCCAAAGGCT	TTTCCTCTGCCGCCAGCCAAAA
Tlr9	GCTGTCAATGGCTCTCAGTTCC	CCTGCAACTGTGGTAGCTCACT
ND1	CTAGCAGAAACAAACCGGGC	CCGGCTGCGTATTCTACGTT
16S	CCGCAAGGGAAAGATGAAAGAC	TCGTTTGGTTTCGGGGTTTC

1

2

3

1 **Table 4:** List of *Gadlor1* and *Gadlor2* probes used for RNA antisense purification (RAP).

	Probe Sequence
***Gadlor1* – Probe 1**	[Btn]AGGATTGTTAAATATGACTATGCTTGGTATAGTCACAAAACATGGGAGTAC
***Gadlor1* – Probe 2**	[Btn]TATCATAATCTTTCTGTAGGCCATTACTTGTTTCATATTTTAAAGGGACAG TCCACTCTAGGAATGTCAAGTGTCTGATCTCTGAAAACA
***Gadlor1* – Probe 3**	[Btn]TTTTCTGAATAGTTGAAAATTCTAACTAAACACAGGAAGAACAGAGNCAC AAGAATAAAGAAATTTAGATATATCCTAAATGTTTCCAGG
***Gadlor1* – Probe 4**	[Btn]ATAAAAGAAGGCGAGGGGTGGCATGCAAGATGATTGAGAAAGCCCAGT AGCCATTTTTGGGGTGGGGCAAAGGGAGTGGTCTGGGTAGGG
***Gadlor2* – Probe 1**	[Btn]GCTGCTATTTTATTATCTCTTTGGTTCTGTTTTTCATTTGTATTAAAAATG
***Gadlor2* – Probe 2**	[Btn]GTGATGGTGAAGATGAAATTGAGATGAATCATTTGAAGAACGATGTGCGTT TTAGAAGAATCACTTTGTC

2

3

4

5

6

7

8

9

10

Supplemental Figure Legends

Supplement Figure 1: *Gadlor1* and *Gadlor2* are non-coding transcripts that are located in the intronic region of the *Lsamp* gene.

A-C. Systemic deletion of the whole region containing *Gadlor* lncRNAs did not affect the expression of the neighbor gene *Lsamp,* which is mainly expressed in brain tissue. (*Gapdh* expression used for normalization) Relative expression of *Gadlor1, Gadlor2* and *Lsamp* were shown in mouse brain, heart and liver tissue samples collected from WT and *Gadlor*-KO mice (n=4, same samples were indicated in each graph).

D. Coding probability of *Gadlor1* and *Gadlor2* was evaluated with the online Coding Potential Assessment Tool (CPAT - http://lilab.research.bcm.edu/), and compared with coding transcripts and well-known lncRNAs for validation that revealed *Gadlor1* and *Gadlor2* are non-coding transcripts.

E-F. Fluorescent *in situ* hybridization of *Gadlor1* (cyan)*, Gadlor2* (red) and *Cdh5 RNAs* in mouse heart tissue sections of **E.** sham and following **F. 8**-weeks of TAC surgery. *Cdh5* shows endothelial cells (green), nuclei stained with DAPI (blue), and the overlap in 3 channels was indicated with arrows. Dashed rectangles were the zoomed areas showed in separate pictures.

Supplement Fig 2: Conservation levels of *Gadlor1/2* between mouse and human genome.

A-B. Assessment between human (H) and mouse (M) *Gadlor1/2* in sequence conservation level evaluated with EMBOSS-Water local alignment tool (https://www.ebi.ac.uk/Tools/psa/emboss_water/)**,** and **C-D.** visualization of pairwise local alignment with LALIGN DNA:DNA tool of University of Virginia (https://fastademo.bioch.virginia.edu/fasta_www2/fasta_www.cgi?rm=lplalign).

Supplement Figure 3: *Gadlor* lncRNAs are mainly secreted in endothelial cells (EC) derived extracellular vesicles (EVs).

A. Scheme depicting the experimental design of EV isolation with ultracentrifugation (UC) from cultured primary cardiac ECs. Characterization of cardiac EC-derived EVs by **B.** visualizing microvesicles and exosomes with electron microscopy (scale bar: 500 nm) and **C.** detecting the size in diameter (nm: nanometers) with Nanoparticle Tracking Analysis (NTA). **D.** Flow cytometry analysis of EV surface markers (CD63-APC, CD9-PerCP-Cy5.5 and CD54-FITC) on EC-derived EVs that were stained against markers (blue curve) and compared to isotype control (red curve). **E.** Expression of *Gadlor1* and *Gadlor2* in C166 mouse endothelial cell and in EVs derived from these cells.

Data are shown as mean±SEM. Data normality was evaluated with Shapiro-Wilk test and p-values were calculated with Student's t-test for parametric (or Mann-Whitney for non-parametric) assessment. *p-value<0.05, **p-value<0.01, ***p-value<0.001.

Supplement Figure 4: Baseline phenotypic characterization of *Gadlor*-KO mice compared to wild-type (WT) littermates.

A. Heart rate of WT and *Gadlor*-KO mice during echocardiography (BPM: beats per minute, n≥12). **B.** Analysis of systolic function parameters of left ventricle (LV) ejection fraction (%), fractional shortening (%), LV posterior wall thickness in diastole (mm) and LV end diastolic volume (µl) (n≥12). **C.** Analysis of diastolic function parameters, global longitudinal strain (GLS, %) and mitral valve (MV) E to E' ratio (n≥4). **D.** Body weight (g) of adult (9 weeks old) WT and *Gadlor*-KO animals (n≥18), and **E.** organ to body weight ratio (mg/g) of isolated organs including heart, lungs, liver, spleen, brain and kidney (n≥8). **F-G.** Representative images and quantification of flow measurement in right and left common carotid arteries

(RCCA and LCCA) in sham (n≥4) and TAC (n≥7) mice to measure the strength of aortic constriction in WT and *Gadlor*-KO animals.

Supplement Figure 5: *Gadlor*-KO mice showed higher mortality despite retaining better structural and physiological remodelling after persisting pressure-overload.

A. Experimental design of long-term TAC operation for *Gadlor*-KO and WT littermates up to 8-weeks after TAC. **B.** Heart weight (mg) to body weight (g) ratio (HW/BW) of *Gadlor*-KO and WT mice in age comparable sham (n≥3) and after 8-weeks TAC (n≥7). **C.** Representative echocardiography images of *Gadlor*-KO and WT mice before (pre-TAC) and after 4-weeks and 8-weels TAC shown in parasternal long axis mode, and analysis of **D.** left ventricle (LV) ejection fraction (EF%) and **E.** left ventricle (LV) posterior wall thickness in diastole (mm), (unpaired analysis)**. F.** Representative immunofluorescence images of cardiac tissue samples stained with WGA (wheat-germ agglutinin coupled with Alexa Fluor 555) and IB4 (Isolectin B4 coupled with Alexa Fluor 488) in sham (n=3) and 8-week TAC (n=5) samples from *Gadlor*-KO and WT littermates, scale-bar: 100 µm. Quantification of **G.** cardiomyocyte cross-sectional area and **H.** myocardial capillary density per cardiomyocyte ratio. **I.** Representative Sirius-red fibrosis staining in cardiac tissue sections of sham (n≥3) and 8-week TAC (n≥6) mice (scale-bar: 1 mm) and **J.** quantification of fibrotic area (%). **K.** Survival of *Gadlor*-KO and WT mice after TAC (n=11). Probability of survival compared with log-rank (Mantel-Cox) test.

Data are shown as mean±SEM. Data normality was evaluated with Shapiro-Wilk test and p-values were calculated with Student's t-test for comparing two groups and two-way ANOVA for grouped analysis followed with Fisher's LSD post-hoc test. *p-value<0.05, **p-value<0.01, ***p-value<0.001, ****p-value<0.0001.

Supplement Figure 6: Deletion of *Gadlor* lncRNAs induces angiogenesis and expression of cell cycle genes in cardiac ECs during pressure-overload.

A. Heatmap showing differentially regulated genes revealed by bulk RNAseq of cardiac endothelial-cells after 2-weeks TAC. **B.** Bar plots showing the gene-ontology (GO) analysis of upregulated and downregulated genes in *Gadlor*-KO ECs compared to WT ECs after 2-weeks TAC (Red: Upregulated in *Gadlor*-KO, Blue: Downregulated in *Gadlor*-KO). Some exemplary genes were listed for selected GO-terms. **C-D.** Validation of selected genes from RNAseq data with qRT-PCR in isolated cardiac ECs after 2 weeks of TAC (Red: Upregulated in *Gadlor*-KO, Blue: Downregulated in *Gadlor*-KO). **E.** Representative immunofluorescence images of cardiac tissue samples stained with IB4 (Isolectin B4 coupled with Alexa Fluor 488) and Ki67 (coupled with Alexa Fluor 555) in 2-week TAC samples from *Gadlor*-KO and WT littermates, Scale bar: 100 µm. (Arrows showing Ki67+ ECs) **F.** Quantification of Ki67 positive endothelial-cells percentage (Ki67+ ECs%). **G.** Representative images of sprouting assay with C166 mouse ECs after adenovirus treatment (Ad*βgal* and Ad*Gadlor1/2*) followed by 24-hour FGF2 or TGFβ treatment. 3-dimentional (3D) collagen matrix embedded spheroids were allowed to form sprouts for 24 hours. Scale bar: 100 µm. **H.** Quantification of average sprout length per spheroid. Data are shown as mean±SEM. Data normality was evaluated with Shapiro-Wilk test. P-values were calculated with Student's t-test for comparing two groups. For grouped analysis, p-values were evaluated with two-way ANOVA followed with Fisher's LSD post-doc test. *p-value<0.05, **p-value<0.01, ***p-value<0.001, ****p-value<0.0001.

Supplement Figure 7: The effects of *Gadlor1/2* overexpression in cardiomyocytes were partially rescued by CaMKII inhibition.

A. Experimental scheme depicting overexpression of *Gadlor1/2* via EC-derived EVs in isolated adult cardiomyocytes (CMs) after 1-week TAC. Control EVs and *Gadlor1/2 EVs* were collected from Ad.βgal and

Ad.*Gadlor1/2* treated C166 ECs, respectively, and incubated with CMs for 4 hours. Samples were treated with KN93 (µM) for 1 hour before contractility and calcium measurements with IonOptix. **B-D.** Sarcomere contractility and calcium transient measurements were recorded in parallel with Multicell HT system with continuous perfusion of basal media on isolated adult CMs after 1-week TAC. Contractility parameters including sarcomere shortening **(B)** and relaxation velocity **(C)**. Calcium decay time constant as an indication of speed of recovery (tau) is shown **(D)**.

Supplement Figure 8: Venn diagrams of differentially expressed genes in different cardiac cell types of *Gadlor*-KO mice compared to WT littermates after 2 weeks of TAC.

A. Venn diagram of upregulated genes in different cardiac cell types (CM: red, EC: grey, FB: blue) of *Gadlor*-KO mice compared to WT after 2-weeks TAC. The numbers indicating the number of genes in corresponding cell types. Genes were filtered as fold-change greater or equals to 1.2 for each condition. **B-E.** Gene ontology (GO) analysis of indicated intersections representing the overlapping upregulated genes in shown cell type of *Gadlor*-KO compared to WT littermates. **F.** Venn diagram of downregulated genes in different cardiac cell types (CM: red, EC: grey, FB: blue) of *Gadlor*-KO mice compared to WT after 2-weeks TAC. **G-J.** Gene ontology (GO) analysis of indicated intersections representing the overlapping downregulated genes in shown cell type of *Gadlor*-KO compared to WT littermates. Bar plots showing selected GO-terms for each condition.

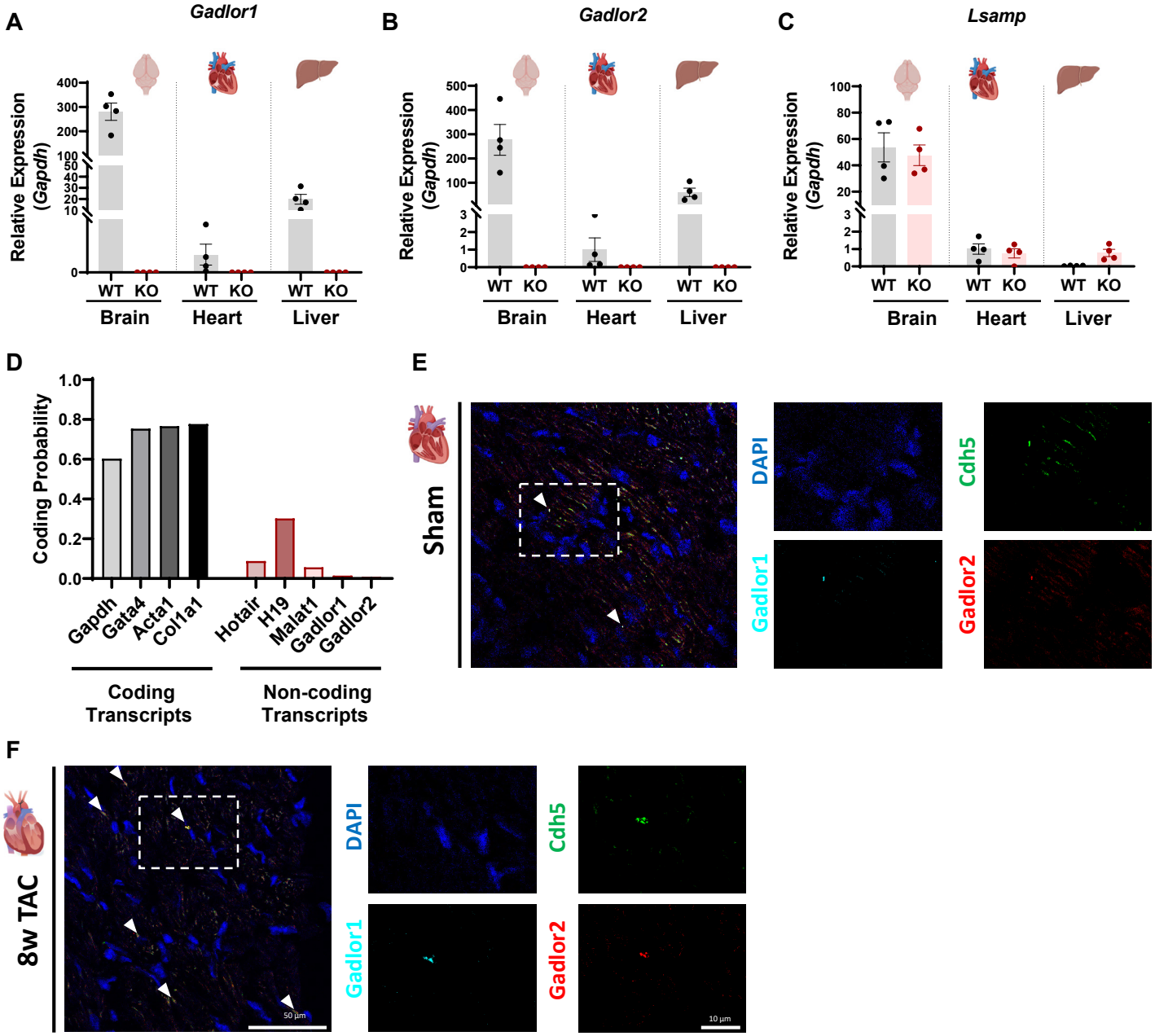

Supplement Figure 1: *Gadlor1* and *Gadlor2* are non-coding transcripts that are located in the intronic region of the *Lsamp* gene.

A-C. Systemic deletion of the whole region containing *Gadlor* lncRNAs did not affect the expression of the neighbor gene *Lsamp,* which is mainly expressed in brain tissue. (*Gapdh* expression used for normalization) Relative expression of *Gadlor1, Gadlor2* and *Lsamp* were shown in mouse brain, heart and liver tissue samples collected from WT and *Gadlor*-KO mice (n=4, same samples were used in each graph).

D. Coding probability of *Gadlor1* and *Gadlor2* was evaluated with the online Coding Potential Assessment Tool (CPAT - http://lilab.research.bcm.edu/), and compared with coding transcripts and well-known lncRNAs for validation that revealed *Gadlor1* and *Gadlor2* are non-coding transcripts.

E-F. Fluorescent *in situ* hybridization of *Gadlor1* (cyan), *Gadlor2* (red) and *Cdh5 RNAs* in mouse heart tissue sections of **E.** sham and following **F. 8**-weeks of TAC surgery. *Cdh5* shows endothelial cells (green), nuclei stained with DAPI (blue), and the overlap in 3 channels was indicated with arrows. Dashed rectangles were the zoomed areas showed in separate pictures.

A **AK037972 (*Gadlor1*)**

```
#=======================================
# Aligned_sequences: 2
# Gap_penalty: 10.0
# Extend_penalty: 0.5
#
# Length: 578
# Identity:     268/578 (46.4%)
# Similarity:   268/578 (46.4%)
# Gaps:         259/578 (44.8%)
# Score: 740.5
#=======================================
H   1 AAATTGTCTAGAA-TGTGGCAGTTTAAAAACACATCTACATTGATCTACA     49
      |||||||.||||| |||||||.|||||||.|||.||..||||||||||.
M   1 AAATTGTTTAGAACTGTGGCACTTTAAAAGCACCTCGGCATTGATCTACT     50

   50 GTCTCAAGGTCCCAC--CTTTGTGTTACTTTTAGAATTTGTAGATGGATG     97
      ..|||.||.||.|||  ||.||||.||||||||||.||||||||||||.
   51 AACTCTAGATCTCACCTCTCTGTGCTACTTTTAGAGTTTGTAGATGGATA    100

   98 TTATTCAGCA-AGGATGACTCATCTACATT-TGGTTTGTCAATTTGTTTT    145
      .|.|.||||| |||| ||.||||||||.|| ||  .||||.|||||||||
  101 CTGTCCAGCAGAGGA-GAGTCATCTACGTTCTG--ATGTCGATTTGTTTT    147

  146 CAAAGATCATA----TGTACATAGCGTCCT----TCGATCTTACTTTCCC    187
      ||.||||||.|    || ||||    ||||    |.|     |||.||||
  148 CAGAGATCAGACACTTG-ACAT----TCCTAGAGTGG-----ACTGTCCC    187

  188 TTTAAAATATGAAACTGATAATGACCTTGAAAAAGAT-------AGAATT    230
      |||||||||||||||...||||||.|||..|.||||||        |.|.||
  188 TTTAAAATATGAAACAAGTAATGGCCTACAGAAAGATTATGATAAAACTT    237

  231 TC----------------------------------------AG------    234
      ||                                        ||
  238 TCCAGTTTTTTGGCTTTTCCCTTCGGCCCTGACTGGATGTGTAGTCTACT    287

  235 --CCACAA--------------------------------------------    240
        ||||||
  288 TCCCACAATCCTGTATGTTACATGGTTCCCTACCCAGACCACTCCCTTTG    337

  241 ----------------------------------------GCATCCCA-    248
                                              ||||.|||
  338 CCCCACCCCAAAAATGGCTACTGGGCTTTCTCAATCATCTTGCATGCCAC    387

  249 ---------------------------------TGAA-------AT----    254
                                       ||||       ||
  388 CCCTCGCCTTCTTTTATGTTTCAGAGTTGTGTGTGAAGAATCACATTAGT    437

  255 --TAATGTATCCATACTTTTAACA--CTA-----GTATAC-----TTTAT    290
        ||.|||||.|.|.||||| |||  |||     ||.|||     |||||
  438 GATACTGTATGCTTTCTTTT-ACAATCTATTTACGTTTACACATATTTAT    486

  291 CTTCTTATTT-CA-AATGCTC--TGTCTCC--------------------    316
      .||..||||| || |.|.|||  |||.|.|
  487 TTTTATATTTACATATTTCTCATTGTTTACCAGTTGGCAATAGTGATATT    536

  317 TT---------CTGTCCA--TTACTTCC    333
      ||         ||.|.||  ||||||||
  537 TTGTGAGCTGACTTTACATTTTACTTCC    564
```

B **AK038629 (*Gadlor2*)**

```
#=======================================
# Aligned_sequences: 2
# Gap_penalty: 10.0
# Extend_penalty: 0.5
#
# Length: 913
# Identity:     656/913 (71.9%)
# Similarity:   656/913 (71.9%)
# Gaps:         130/913 (14.2%)
# Score: 2336.5
#=======================================
H   1 AAAAAGAAAATTTGGA-AGATGCTCAAATAGGA-TTGATAGAGGTTCATT     48
      ||.||.||||||||| || |||.||.|||||| ||| .||.|..|||..
M  34 AAGAATAAAATTTGGACAG-TGCACACATAGGACTTG-CAGGGACTCACA     81

   49 TTGTGTCATATTTT-CGCTTTATATGGATGTTGATATGTTCTCAGAATAA     97
      .||||||||||||| |.||||.||||.||||||||||||.||||||| |
   82 GTGTGTCATATTTTGCACTTTTTATGAATGTTGATATGTTTTCAGAAT-A    130

   98 ATTTATAACTGCAATAGAAAATGGAATGACTATTGATTATTTTTTAGTTA    147
      ||||||||||||||.|||||..|||||.||||||||||..||||||||.
  131 ATTTATAACTGCAATTGAAAACTGAATGGCTATTGATTAAATTTTAGTTT    180

  148 CCCAAACTAATTGTCATATAAAGCTTTGTAAAT-CTTTTA-AAATGAGTA    195
      |..|||||||||.||||||||||||..||||| |||||| |||  ||.|
  181 CAAAAACTAATTGACATATAAAGCTTCATAAATCCTTTTAGAAA--AGGA    228

  196 TGGGTGTAAATTAAAAACGAATTAAAGCAGAGGCTTATAAAGACACT---    242
      ||.||.||||||||||||.|||||.||||.||||||||||| |.|||
  229 TGAGTATAAATTAAAAACTAATTACAGCAAAGGCTTATAAA-ATACTCCA    277

  243 ATCTCCCCTTCAATGGGTTATGTATTTTTGTTGTGTGTTAGGAAGATATC    292
      || |||..|||.|| ||||||.||   .||||||.||.||.||||.|.|.
  278 AT-TCCAGTTCTAT-GGTTATATA---CTGTTGTATGCTATGAAGGTGTT    322

  293 TCTTGATCTCCACACCCAAAACTCCTTCC----------AAATGAACAAA    332
      .|||..|||.|..|..||||||||||.||          |.||||||
  323 CCTTTGTCTTCTTAATCAAAACTCCTGCCATAGAATTAAATATGAAC---    369

  333 GGCCTACACACAAAAATTATTTCAATTGCTAATAGCCAGTTTTTAT----    378
            ||.||||..||||.||||||||||....|.|||.|||
  370 --------CATAAAAGATATTTTAATTGCTAATGATTACTTTATATATAG    411

  379 ------TTTTCAAAAGTAAATGCTTTCTTTTTTTGAAAAGTAAATATAAC    422
            |||||||.||                     |||  .|||||.
  412 TATCCCTTTTCAAGAG----------------------AGT--TTATAAG    437

  423 TATTTTAACAAAGTAAGATTTAAAAA---AAAAAACAACTCAGAAAAAAG    469
      .|||||.|...|||||.|||||||||   ||||||.|||      |.|||
  438 AATTTTTAATCAGTAATATTTAAAAATTTAAAAAAGAAC------AGAAG    481

  470 T--GCCAT------GCAG-AGATAACAGGGCTGATCTGTCTGTTATCTGC    510
      |  |||||      |||| ||| |.||      || ||.|.||||||||.
  482 TGGGCCATGTTAAGGCAGCAGA-ACCA------AT-TGCCAGTTATCTGT    523

  511 AGCCTCTATCCTTACTGTTAACAAGCCTTTTATCTTTGAAGACACTAAAC    560
      |.||||||||||..||.|||.||||||||||.|||.||||||||||||.|
  524 AACCTCTATCCTTGATGCTAATAAGCCTTTTACCTTCGAAGACACTAAGC    573

  561 ATCTGGGATCTAAGCACTGACACCTATTAGTTACAGTGGTTTCCTTTTAC    610
      ||||||||||||||.|.||||||||||||||||||.||||||||||||||
  574 ATCTGGGATCTAAGTAGTGACACCTATTAGTTACAATGGTTTCCTTTTAC    623

  611 CTTTCTAAACTATCTGATAGATAAACCTCCAGGAATCCTACAAAATTAGG    660
      | ||||||.|.||||||||||||||||||||||||||||.||||||||.|.
  624 C-TTCTAAGCAATCTGATAGATAAACCTCCAGGAATCCCACAAAATTGGA    672

  661 CCCTTAATTGACCAAACGAATGTCTGTCTCTCTTTTTCAATCTAAATCAA    710
      ||||||||||||||||.||||||.||||||||||||||.||.|.||||||..|
  673 CCCTTAATTGACCAAATGAATGGCTGTCTCTCTTTTACAGTATAAATTGA    722

  711 AAAG-GAGTTTGCTCCTAGGAG--ATGAGATGATGTACAGTGGAAAAAAA    757
      |||| ||||||||||.|.|||  |.||.||.|..||    |||||.|||
  723 AAAGTGAGTTTGCTCCCATGAGGTAAGACATAACTTA----GGAAAGAAA    768

  758 TATTTCA-GCTGCAACTCCACTGGTAACCGTCAATGTGACCTTATAATCT    806
          ||| ||||..||||||||.|..| |.|.|.||||.||||.||||||
  769 ----TCACGCTGAGACTCCACTTGCCA-CATTAGTGTGCCCTTGTAATCT    813

  807 CCCC-----CCAATTTATTCCCA-AAACAGCTA--CCAAAGTGATCTTTC    848
      |.||     |||       |||| .||||| ||  .|||||||||..|||
  814 CACCAAAAGCCA-------CCCACCAACAG-TAGGACAAAGTGATTCTTC    855

  849 TAAAACCCACATC    861
      ||||||.||||||
  856 TAAAACGCACATC    868
```

C

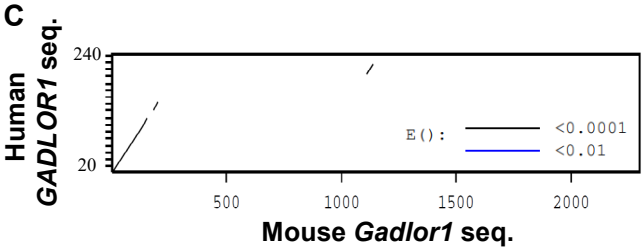

D

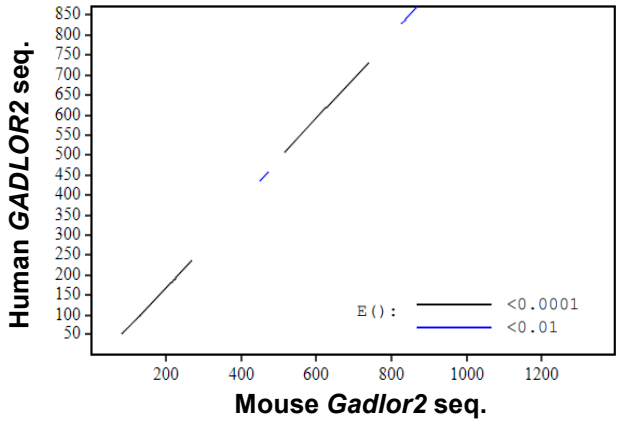

Supplement Fig 2: Conservation levels of *Gadlor1/2* between mouse and human genome.

A-B. Assessment between human (H) and mouse (M) *Gadlor1/2* in sequence conservation level evaluated with EMBOSS-Water local alignment tool (https://www.ebi.ac.uk/Tools/psa/emboss_water/), and **C-D.** visualization of pairwise local alignment with LALIGN DNA:DNA tool of University of Virginia (https://fastademo.bioch.virginia.edu/fasta_www2/fasta_www.cgi?rm=lplalign).

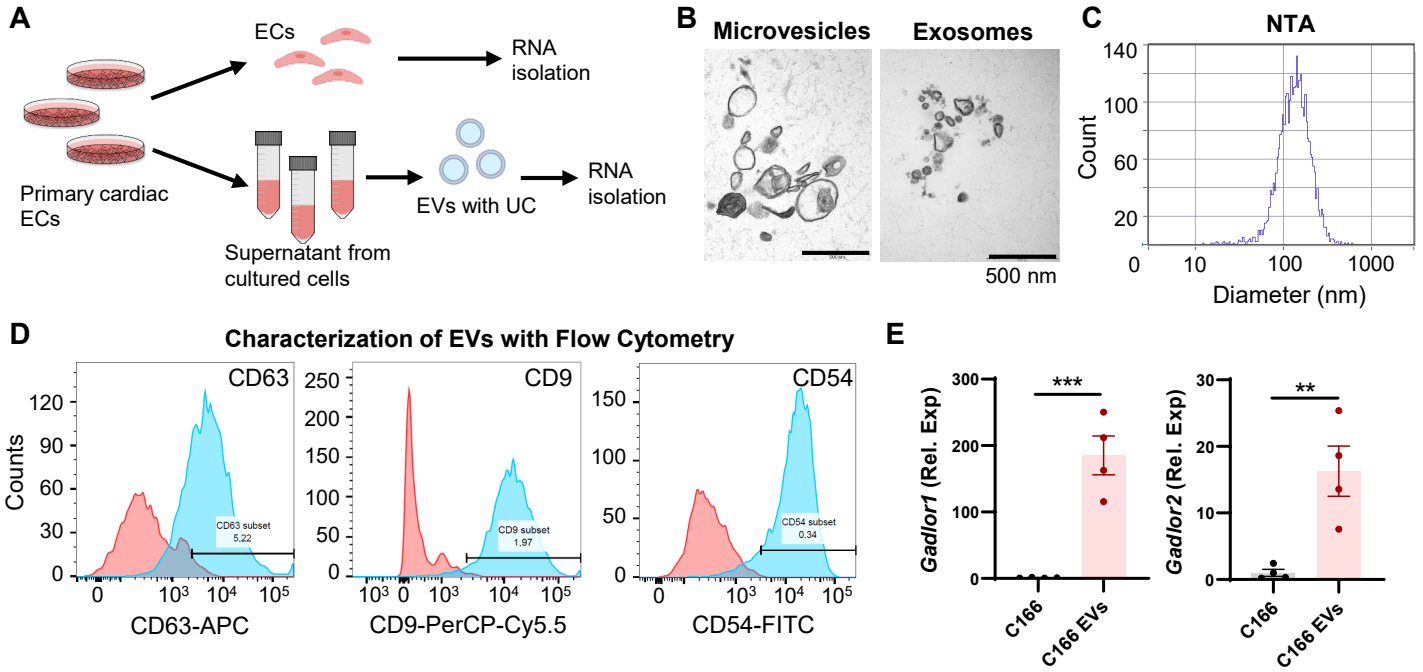

Supplement Figure 3: *Gadlor* lncRNAs are mainly secreted in endothelial cells (EC) derived extracellular vesicles (EVs).

A. Scheme depicting the experimental design of EV isolation with ultracentrifugation (UC) from cultured primary cardiac ECs. Characterization of cardiac EC-derived EVs by **B.** visualizing microvesicles and exosomes with electron microscopy (scale bar: 500 nm) and **C.** detecting the size in diameter (nm: nanometers) with Nanoparticle Tracking Analysis (NTA). **D.** Flow cytometry analysis of EV surface markers (CD63-APC, CD9-PerCP-Cy5.5 and CD54-FITC) on EC-derived EVs that were stained against markers (blue curve) and compared to isotype control (red curve). **E.** Expression of *Gadlor1* and *Gadlor2* in C166 mouse endothelial cell and in EVs derived from these cells.
Data are shown as mean±SEM. Data normality was evaluated with Shapiro-Wilk test and p-values were calculated with Student's t-test for parametric (or Mann-Whitney for non-parametric) assessment. *p-value<0.05, **p-value<0.01, ***p-value<0.001.

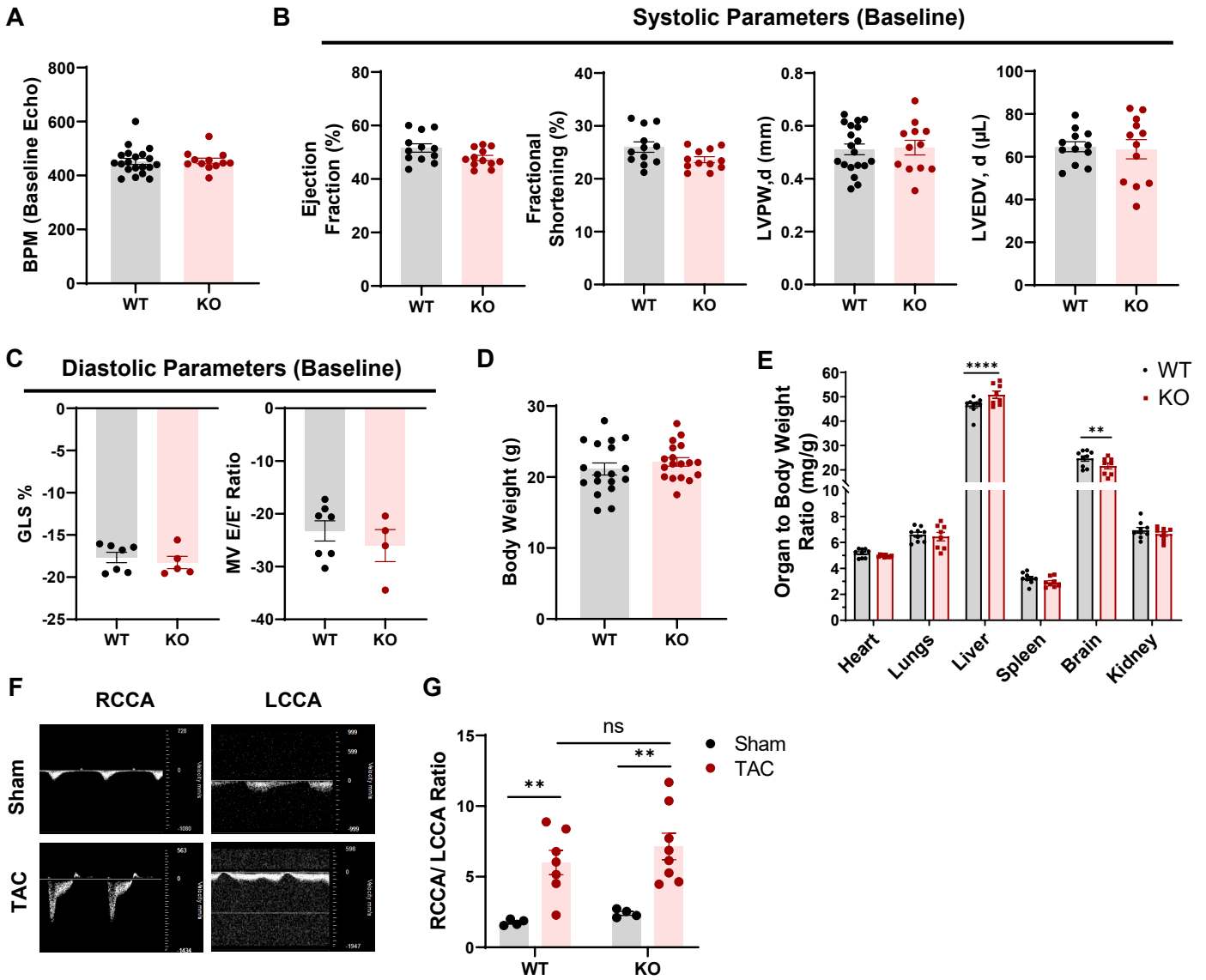

Supplement Figure 4: Baseline phenotypic characterization of *Gadlor*-KO mice compared to wild-type (WT) littermates.

A. Heart rate of WT and *Gadlor*-KO mice during echocardiography (BPM: beats per minute, n≥12). **B.** Analysis of systolic function parameters of left ventricle (LV) ejection fraction (%), fractional shortening (%), LV posterior wall thickness in diastole (mm) and LV end diastolic volume (µl) (n≥12). **C.** Analysis of diastolic function parameters, global longitudinal strain (GLS, %) and mitral valve (MV) E to E' ratio (n≥4). **D.** Body weight (g) of adult (9 weeks old) WT and *Gadlor*-KO animals (n≥18), and **E.** organ to body weight ratio (mg/g) of isolated organs including heart, lungs, liver, spleen, brain and kidney (n≥8). **F-G.** Representative images and quantification of flow measurement in right and left common carotid arteries (RCCA and LCCA) in sham (n≥4) and TAC (n≥7) mice to measure the strength of aortic constriction in WT and *Gadlor*-KO animals.

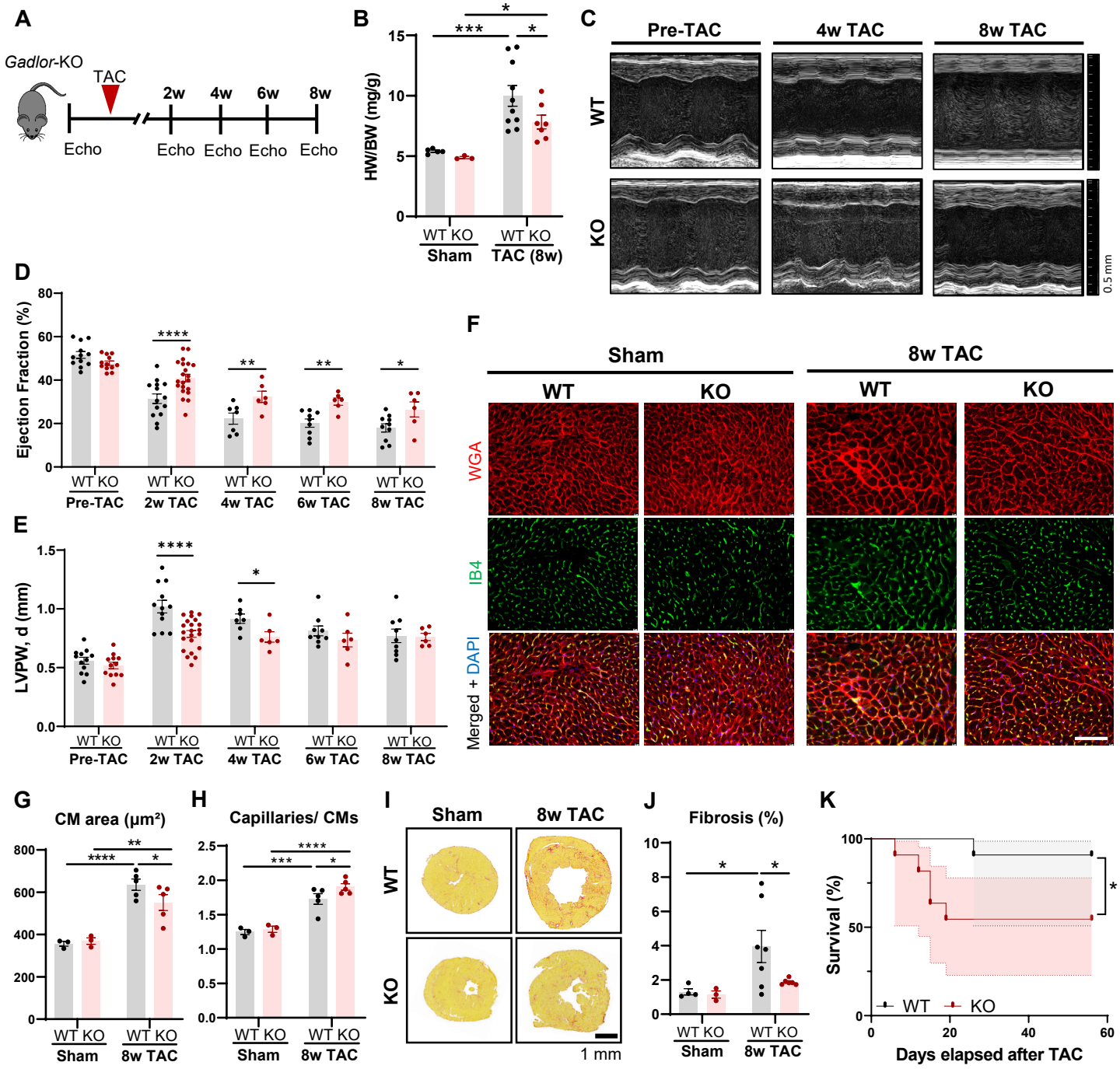

Supplement Figure 5: *Gadlor*-KO mice showed higher mortality despite retaining better structural and physiological remodelling after persisting pressure-overload.

A. Experimental design of long-term TAC operation for *Gadlor*-KO and WT littermates up to 8-weeks after TAC. **B.** Heart weight (mg) to body weight (g) ratio (HW/BW) of *Gadlor*-KO and WT mice in age comparable sham (n≥3) and after 8-weeks TAC (n≥7). **C.** Representative echocardiography images of *Gadlor*-KO and WT mice before (pre-TAC) and after 4-weeks and 8-weels TAC shown in parasternal long axis mode, and analysis of **D.** left ventricle (LV) ejection fraction (EF%) and **E.** left ventricle (LV) posterior wall thickness in diastole (mm), (unpaired analysis)**. F.** Representative immunofluorescence images of cardiac tissue samples stained with WGA (wheat-germ agglutinin coupled with Alexa Fluor 555) and IB4 (Isolectin B4 coupled with Alexa Fluor 488) in sham (n=3) and 8-week TAC (n=5) samples from *Gadlor*-KO and WT littermates, scale-bar: 100 µm. Quantification of **G.** cardiomyocyte cross-sectional area and **H.** myocardial capillary density per cardiomyocyte ratio. **I.** Representative Sirius-red fibrosis staining in cardiac tissue sections of sham (n≥3) and 8-week TAC (n≥6) mice (scale-bar: 1 mm) and **J.** quantification of fibrotic area (%). **K.** Survival of *Gadlor*-KO and WT mice after TAC (n=11). Probability of survival compared with log-rank (Mantel-Cox) test.
Data are shown as mean±SEM. Data normality was evaluated with Shapiro-Wilk test and p-values were calculated with Student's t-test for comparing two groups and two-way ANOVA for grouped analysis followed with Fisher's LSD post-hoc test. *p-value<0.05, **p-value<0.01, ***p-value<0.001, ****p-value<0.0001.

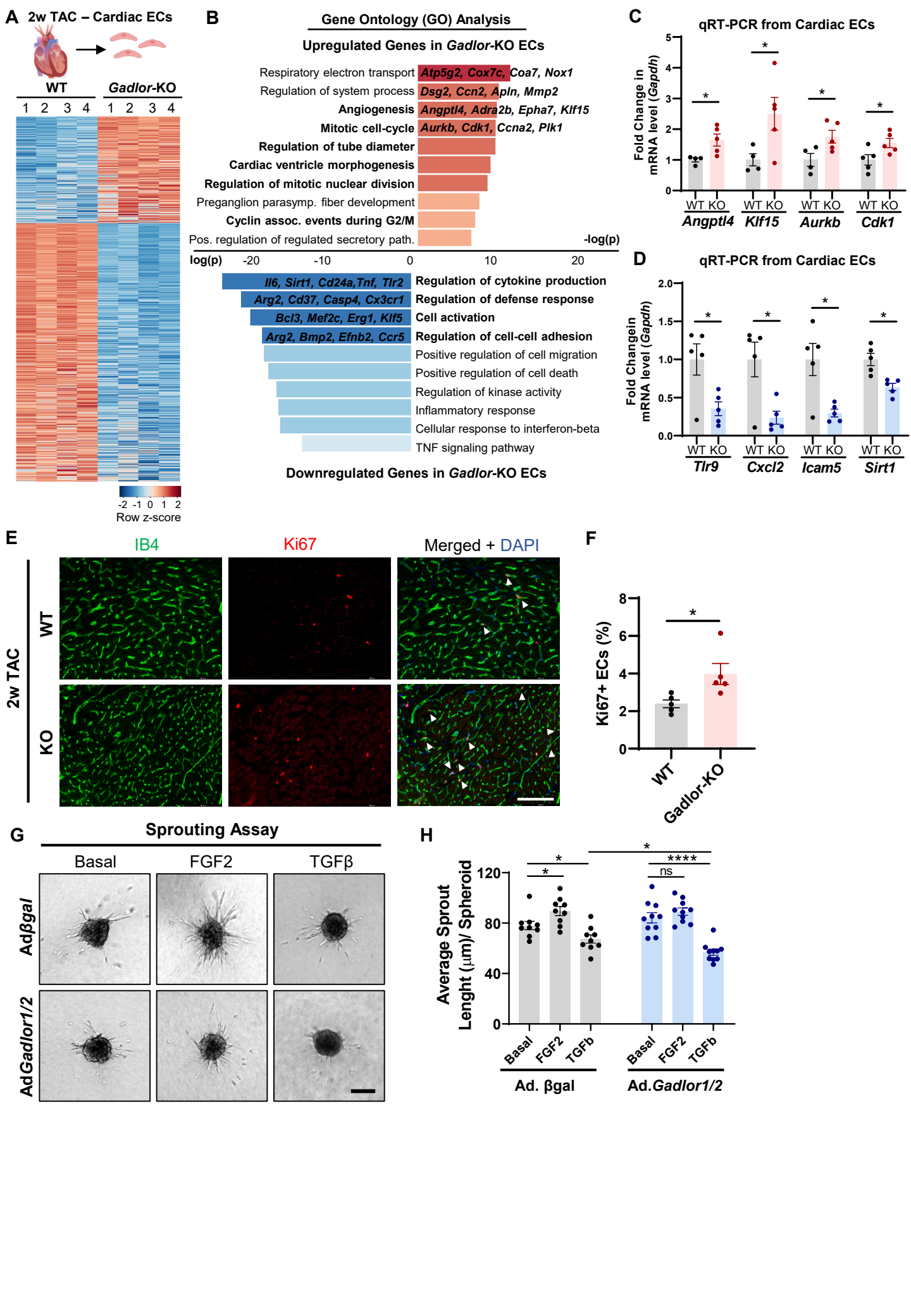
A
2w TAC – Cardiac ECs
WT
Gadlor-KO
1 2 3 4
1 2 3 4
-2 -1 0 1 2
Row z-score
B
Gene Ontology (GO) Analysis
Upregulated Genes in Gadlor-KO ECs
Respiratory electron transport
Atp5g2, Cox7c, Coa7, Nox1
Regulation of system process
Dsg2, Ccn2, Apln, Mmp2
Angiogenesis
Angptl4, Adra2b, Epha7, Klf15
Mitotic cell-cycle
Aurkb, Cdk1, Ccna2, Plk1
Regulation of tube diameter
Cardiac ventricle morphogenesis
Regulation of mitotic nuclear division
Preganglion parasymp. fiber development
Cyclin assoc. events during G2/M
Pos. regulation of regulated secretory path.
-log(p)
log(p) -20 -10 0 10 20
Il6, Sirt1, Cd24a,Tnf, Tlr2
Regulation of cytokine production
Arg2, Cd37, Casp4, Cx3cr1
Regulation of defense response
Bcl3, Mef2c, Erg1, Klf5
Cell activation
Arg2, Bmp2, Efnb2, Ccr5
Regulation of cell-cell adhesion
Positive regulation of cell migration
Positive regulation of cell death
Regulation of kinase activity
Inflammatory response
Cellular response to interferon-beta
TNF signaling pathway
Downregulated Genes in Gadlor-KO ECs
C
qRT-PCR from Cardiac ECs
Fold Change in mRNA level (Gapdh)
WT KO
Angptl4
Klf15
Aurkb
Cdk1
D
qRT-PCR from Cardiac ECs
Fold Changein mRNA level (Gapdh)
Tlr9
Cxcl2
Icam5
Sirt1
E
IB4
Ki67
Merged + DAPI
2w TAC
WT
KO
F
Ki67+ ECs (%)
WT
Gadlor-KO
G
Sprouting Assay
Basal
FGF2
TGFβ
Adβgal
AdGadlor1/2
H
Average Sprout Lenght (μm)/ Spheroid
Basal
FGF2
TGFb
Ad. βgal
Ad.Gadlor1/2
ns
****

Supplement Figure 6: Deletion of *Gadlor* lncRNAs induces angiogenesis and expression of cell cycle genes in cardiac ECs during pressure-overload.

A. Heatmap showing differentially regulated genes revealed by bulk RNAseq of cardiac endothelial-cells after 2-weeks TAC. **B.** Bar plots showing the gene-ontology (GO) analysis of upregulated and downregulated genes in *Gadlor*-KO ECs compared to WT ECs after 2-weeks TAC (Red: Upregulated in *Gadlor*-KO, Blue: Downregulated in *Gadlor*-KO). Some exemplary genes were listed for selected GO-terms. **C-D.** Validation of selected genes from RNAseq data with qRT-PCR in isolated cardiac ECs after 2 weeks of TAC (Red: Upregulated in *Gadlor*-KO, Blue: Downregulated in *Gadlor*-KO). **E.** Representative immunofluorescence images of cardiac tissue samples stained with IB4 (Isolectin B4 coupled with Alexa Fluor 488) and Ki67 (coupled with Alexa Fluor 555) in 2-week TAC samples from *Gadlor*-KO and WT littermates, Scale bar: 100 µm. (Arrows showing Ki67+ ECs) **F.** Quantification of Ki67 positive endothelial-cells percentage (Ki67+ ECs%). **G.** Representative images of sprouting assay with C166 mouse ECs after adenovirus treatment (Ad*βgal* and Ad*Gadlor1/2*) followed by 24-hour FGF2 or TGFβ treatment. 3-dimentional (3D) collagen matrix embedded spheroids were allowed to form sprouts for 24 hours. Scale bar: 100 µm. **H.** Quantification of average sprout length per spheroid. Data are shown as mean±SEM. Data normality was evaluated with Shapiro-Wilk test. P-values were calculated with Student's t-test for comparing two groups. For grouped analysis, p-values were evaluated with two-way ANOVA followed with Fisher's LSD post-doc test. *p-value<0.05, **p-value<0.01, ***p-value<0.001, ****p-value<0.0001.

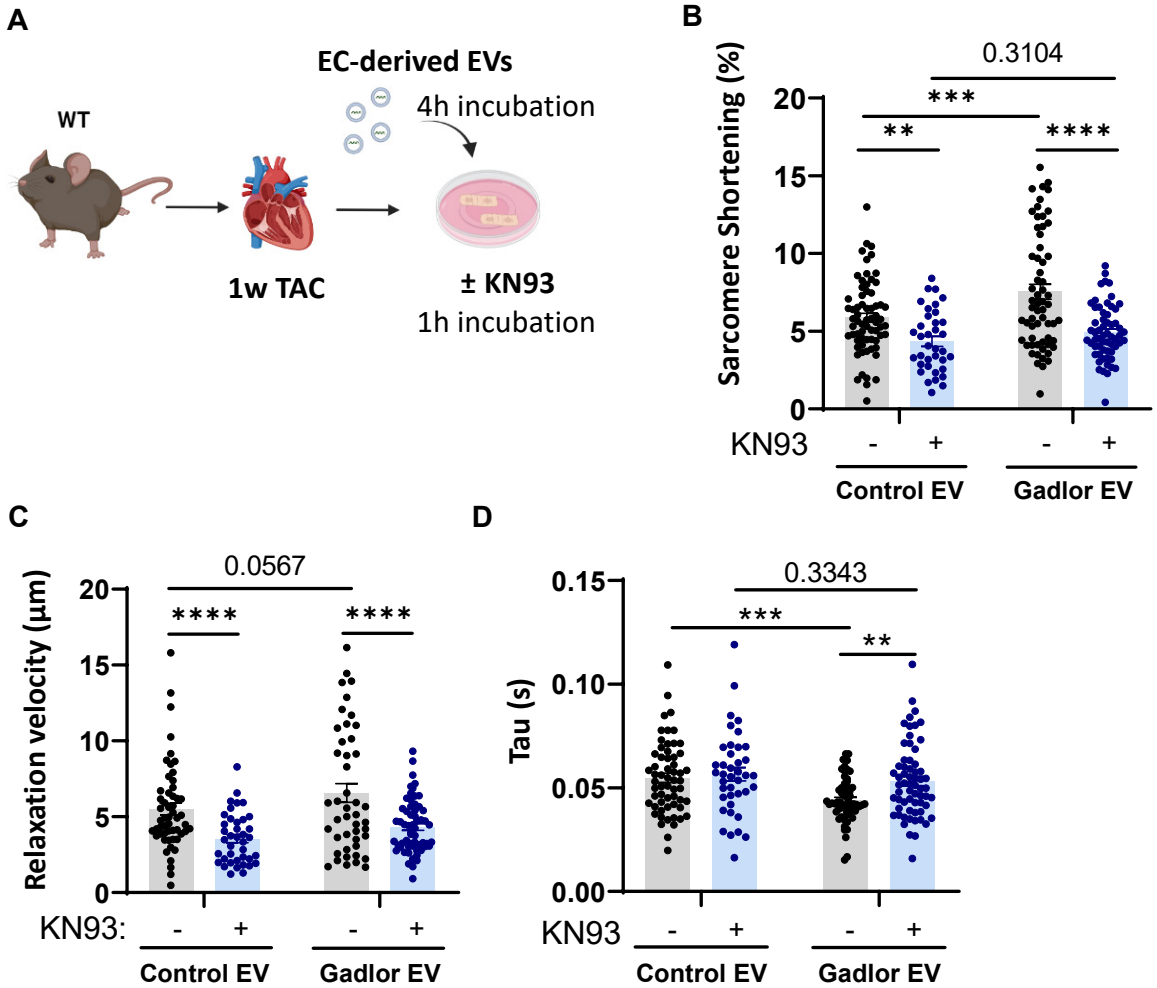

Supplement Figure 7: The effects of *Gadlor1/2* overexpression in cardiomyocytes were partially rescued by CaMKII inhibition.

A. Experimental scheme depicting overexpression of *Gadlor1/2* via EC-derived EVs in isolated adult cardiomyocytes (CMs) after 1-week TAC. Control EVs and *Gadlor1/2 EVs* were collected from Ad.βgal and Ad.*Gadlor1/2* treated C166 ECs, respectively, and incubated with CMs for 4 hours. Samples were treated with KN93 (µM, CaMKII inhibitor) for 1 hour before contractility and calcium measurements with IonOptix. **B-D.** Sarcomere contractility and calcium transient measurements were recorded in parallel with Multicell HT system with continuous perfusion of basal media on isolated adult CMs after 1-week TAC. Contractility parameters including sarcomere shortening **(B)** and relaxation velocity **(C)**. Calcium decay time constant as an indication of speed of recovery (tau) is shown **(D)**.

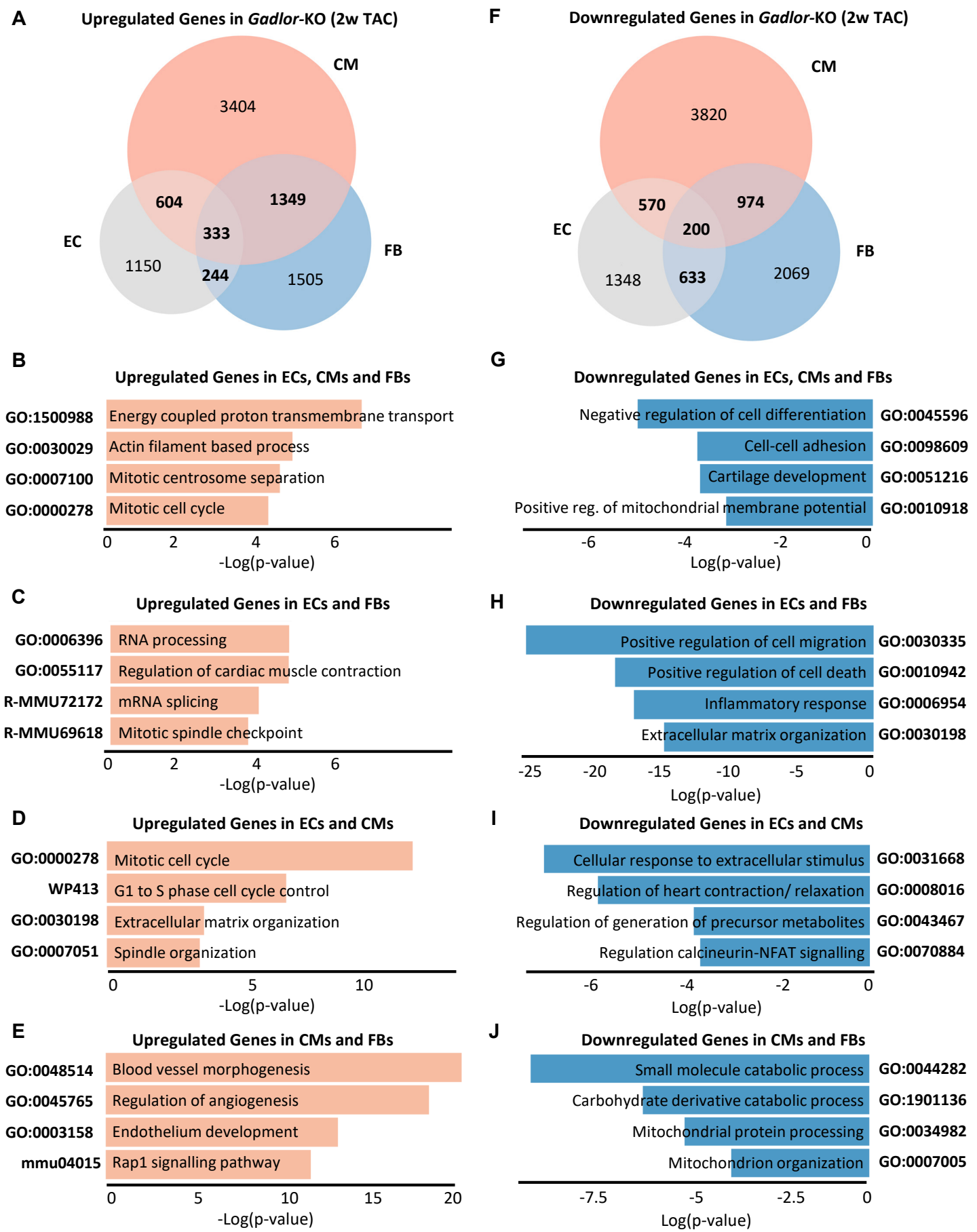

Supplement Figure 8: Venn diagrams of differentially expressed genes in different cardiac cell types of *Gadlor*-KO mice compared to WT littermates after 2 weeks of TAC.

A. Venn diagram of upregulated genes in different cardiac cell types (CM: red, EC: grey, FB: blue) of *Gadlor*-KO mice compared to WT after 2-weeks TAC. The numbers indicating the number of genes in corresponding cell types. Genes were filtered as fold-change greater or equals to 1.2 for each condition. **B-E.** Gene ontology (GO) analysis of indicated intersections representing the overlapping upregulated genes in shown cell type of *Gadlor*-KO compared to WT littermates. **F.** Venn diagram of downregulated genes in different cardiac cell types (CM: red, EC: grey, FB: blue) of *Gadlor*-KO mice compared to WT after 2-weeks TAC. **G-J.** Gene ontology (GO) analysis of indicated intersections representing the overlapping downregulated genes in shown cell type of *Gadlor*-KO compared to WT littermates. Bar plots showing selected GO-terms for each condition.

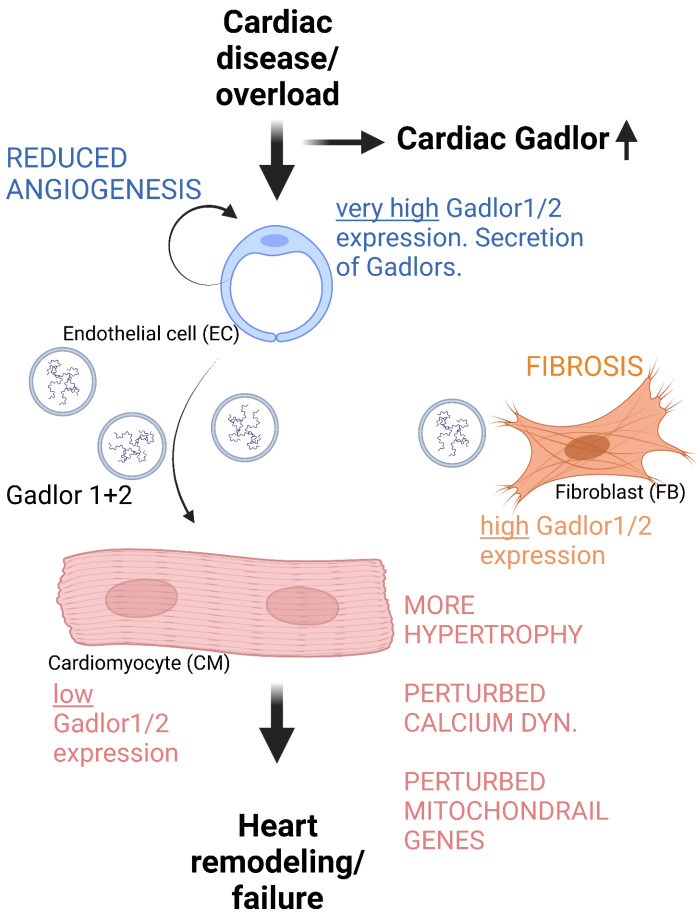

Graphical summary showing *Gadlor1* and *Gadlor2* lncRNAs expression and their effects (capitalized letters). The illustration was created with BioRender.com.